NTNU
Norwegian University of
Science and Technology

Use of SED approach to predict the fatigue behaviour of Aluminium V-Notched Samples

Omar Shihadeh

Mechanical Engineering
Submission date: August 2018
Supervisor: Filippo Berto, MTP
Co-supervisor: Luigi Viespoli, MTP

Norwegian University of Science and Technology
Department of Mechanical and Industrial Engineering

Contents

ABSTRACT 3

1. COMPUTATION OF STRAIN ENERGY DENSITY FOR V-NOTCHED ALUMINUM SAMPLES 4
2. DIFFERENCE BETWEEN ELASTIC AND PLASTIC MODEL 11
3. COMPUTATION OF THE NOTCH STRESS INTENSITY FACTOR 19
4. DIMENSIONLESS PARAMETER Y 24
5. INITIATION AND PROPAGATION OF THE CRACK 26
6. HAIGH DIAGRAM 31
7. EQUIVALENT METHOD TO CHARACTERIZE THE FATIGUE BEHAVIOR OF THE ALUMINUM SPECIMEN 39
8. CONCLUSION 45

BIBLIOGRAPHY 47

Abstract

The aim of the work is that of using SED approach to predict the fatigue behavior of the aluminum alloy 6082-T6. The following steps are made in order to develop the model necessary to do reach this goal:

1. Fatigue tests of 15 aluminum V-notched specimens;
2. Implementation of the elastic model and plot of the Wöhler curves using SED;
3. Analysis of the differences between elastic and plastic models, developed using the FEM software Ansys;
4. Computation of the Notch Stress Intensity Factor using SED and stress and comparison of the numerical values;
5. Computation of the number of cycles necessary to nucleate and propagate the crack;
6. Plot of the Haigh diagrams using SED;
7. Use of the equivalent stress and SED, computed using Gerber and Goodman`s relation.

1. Computation of Strain Energy Density for V-Notched Aluminum Samples

A static linear analysis has been performed, using the Ansys® APDL code, to compute the value of SED around the V-shaped notch's tip. It has been used a plane183 element in condition of plain strain. In the table below are reported the relevant value of the 6082-T6 aluminum alloy of the sample.

E [MPa]	$\boldsymbol{\nu}$	$\boldsymbol{\sigma_R}$ **[MPa]**
64000	0,34	275

The critical radius is assumed equal to that of the welded aluminum, which can be found in literature and it is equal to 0.12 mm (1). The geometry of the sample is reported in the following figure

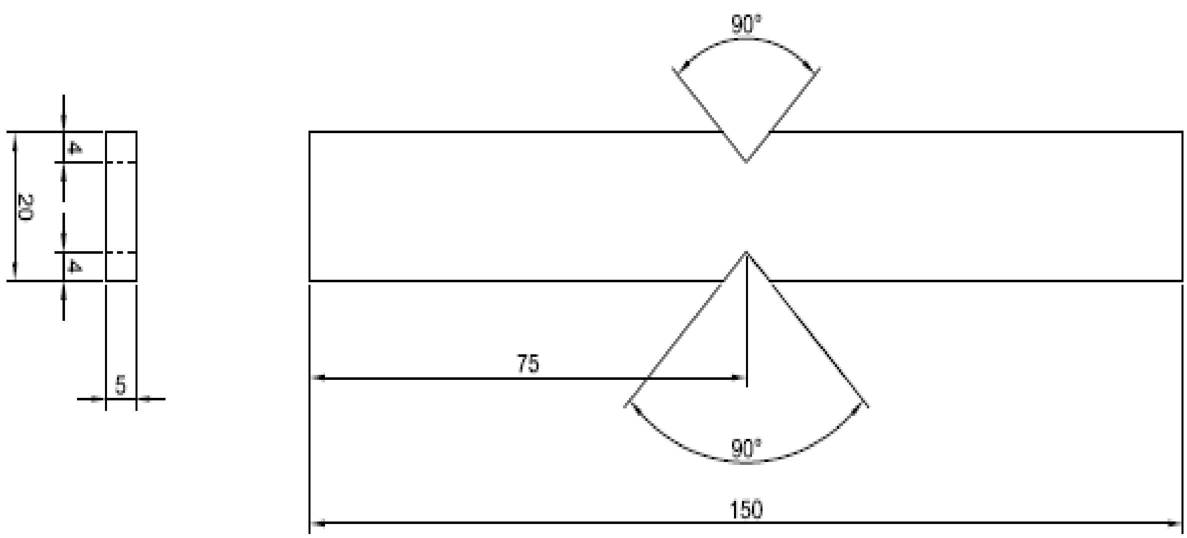

FIGURE 1 GEOMETRY OF THE SPECIMEN

In the Ansys' model the specimen has been loaded to ensure a tension $\Delta\sigma_1$ of 1 MPa at the restricted area.

The averaged SED value on the control volume can be computed simply by dividing two outputs of the model

$$W = \frac{SENE}{VOLU}$$

In which SENE is the strain energy of the control volume and VOLU is the volume inside the critical radius.

As it is shown in the table and in the figure below, coarse mesh in enough to compute a precise value of SED. Singular elements around the notch's tip have been used, thanks to the command KSCON, which allows to move the nodes on the radial sides of the element at a quarter of the side length from the concentration point.

elements	**volu [mm^3]**	**sene [N·mm]**	**ΔW_1 [N·mm/mm^3]**
142	1,696E-02	1,733E-06	1,021E-04
508	1,696E-02	1,725E-06	1,017E-04
1098	1,696E-02	1,725E-06	1,017E-04

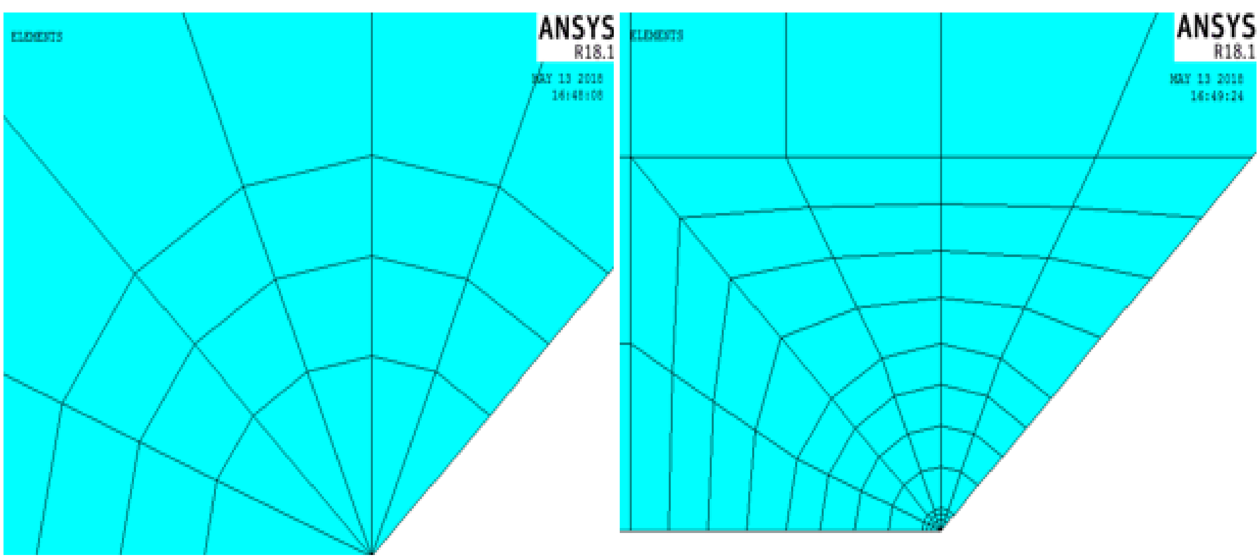

FIGURE 2 CRITICAL AREA (SX) AND MESH OF THE MODEL (DX)

Using the following expression, it is possible to evaluate the value of SED for each test and to plot its value in function of the number of cycles

$$\frac{\Delta W_1}{\Delta W_2} = \left(\frac{\Delta\sigma_1}{\Delta\sigma_2}\right)^2$$

The Wöhler curve and the data for the two series of specimens with load ratio equal to 0 and 0.5 are

σ_{max} [MPa]	N [cycle]	ΔW [N·mm/mm³]
40	RUN OUT	0,163
50	511426	0,254
50	532025	0,254
60	270174	0,366
60	298772	0,366
80	59360	0,651
80	86392	0,651
100	34745	1,017
100	35148	1,017
120	16360	1,465
120	16856	1,465

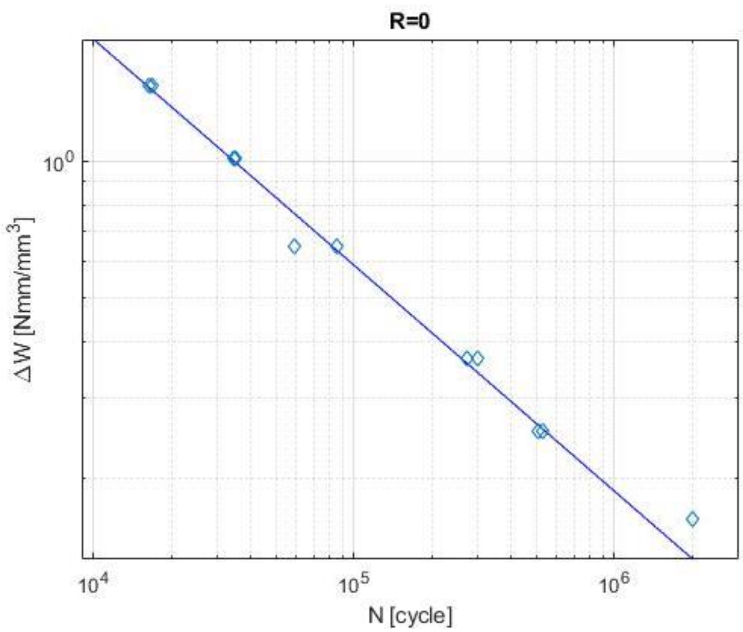

FIGURE 3 WÖHLER CURVE OF THE SPECIMENS LOADED WITH R=0

σ_{max} [MPa]	N [cycle]	ΔW [N·mm/mm^3]
60	2000000	0,092
80	653514	0,163
120	116732	0.366
140	54631	0.498

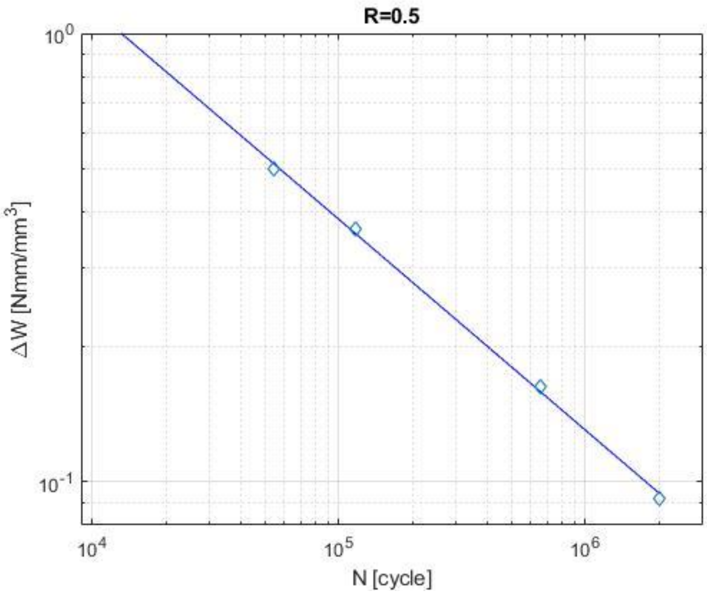

FIGURE 4 WÖHLER CURVE OF THE SPECIMENS LOADED WITH R=0.5

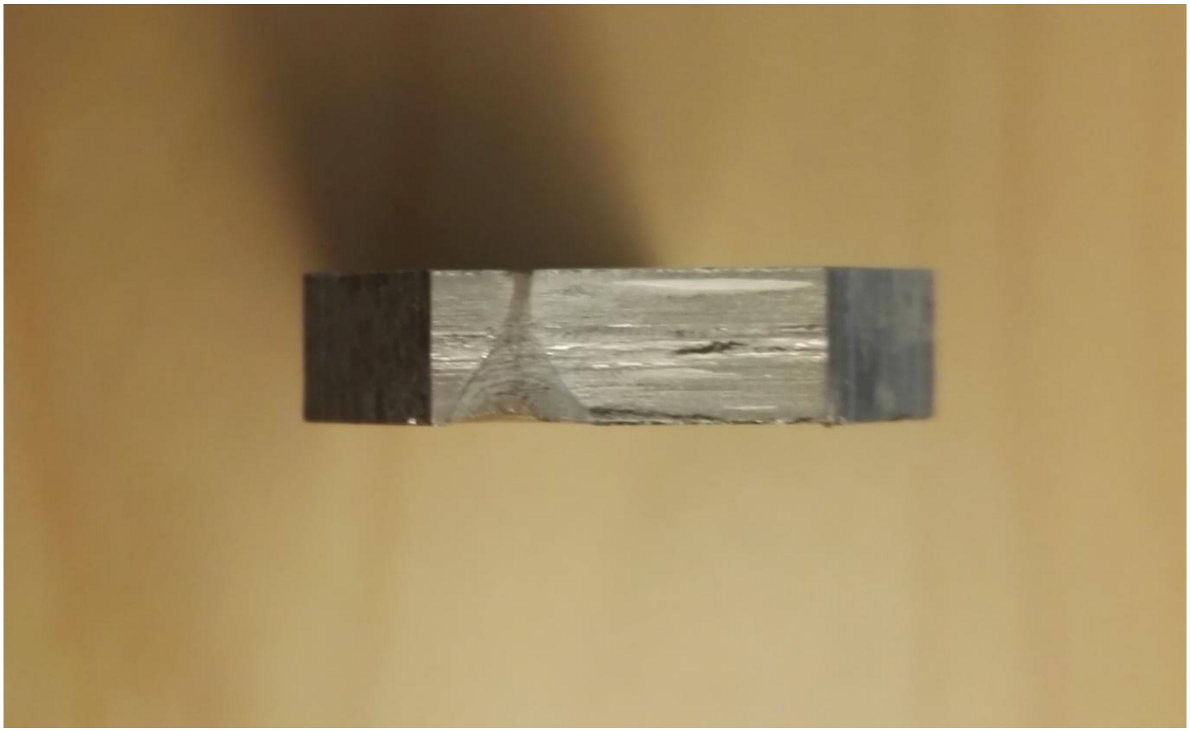

FIGURE 5 SPECIMEN 12, MAX LOAD 50 MPA, FATIGUE LIFE 511426 CYCLES, R=0

FIGURE 6 SPECIMEN 16,MAX LOAD 50 MPA, FATIGUE LIFE 532025 CYCLES, R=0

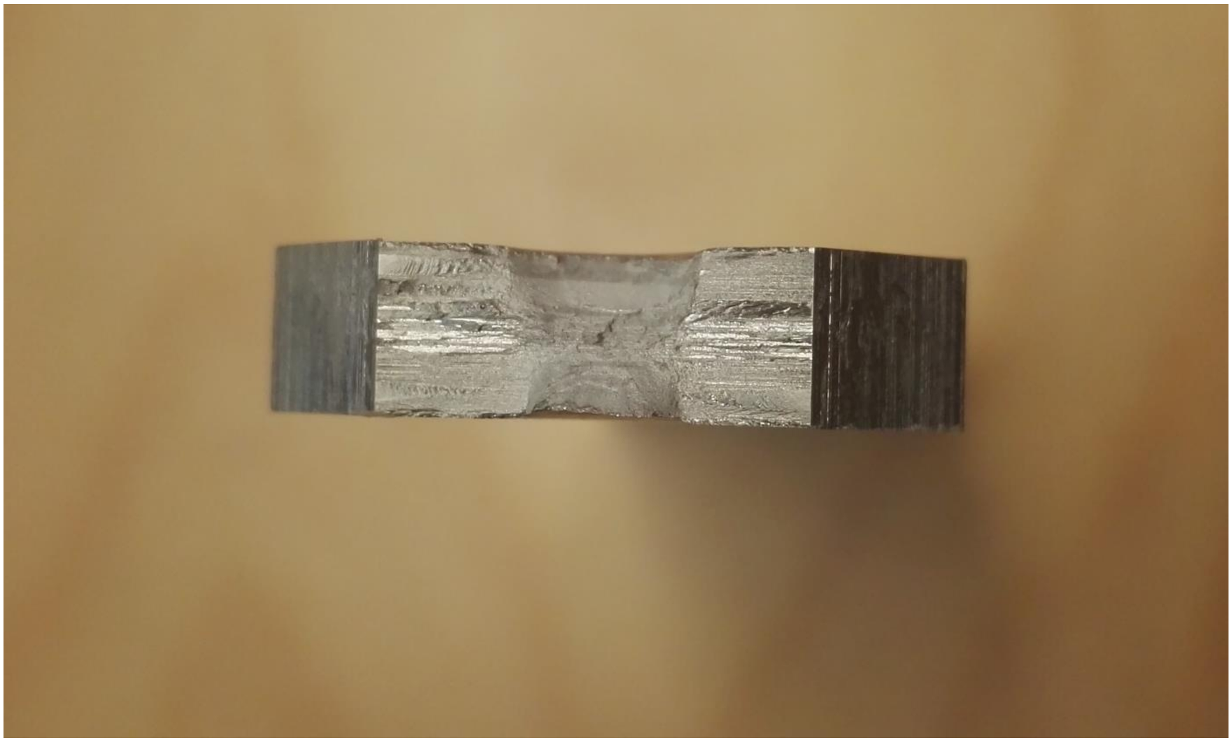

FIGURE 7 SPECIMEN 11, MAX LOAD 120 MPA, FATIGUE LIFE 16856 CYCLES, R=0

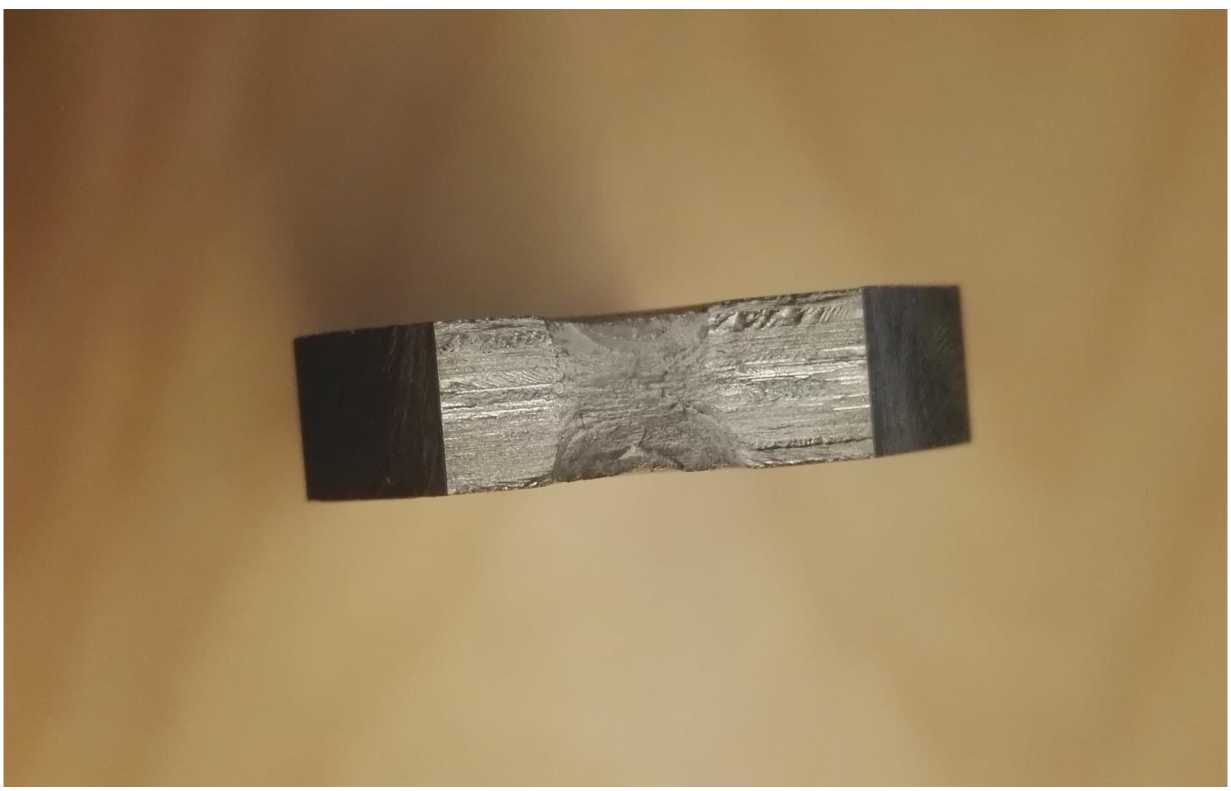

FIGURE 8 SPECIMEN 2, MAX LOAD 120 MPA, FATIGUE LIFE 16360 CYCLES, R=0

FIGURE 9 SPECIMEN 14, MAX LOAD 80 MPA, FATIGUE LIFE 653514 CYCLES, R=0.5

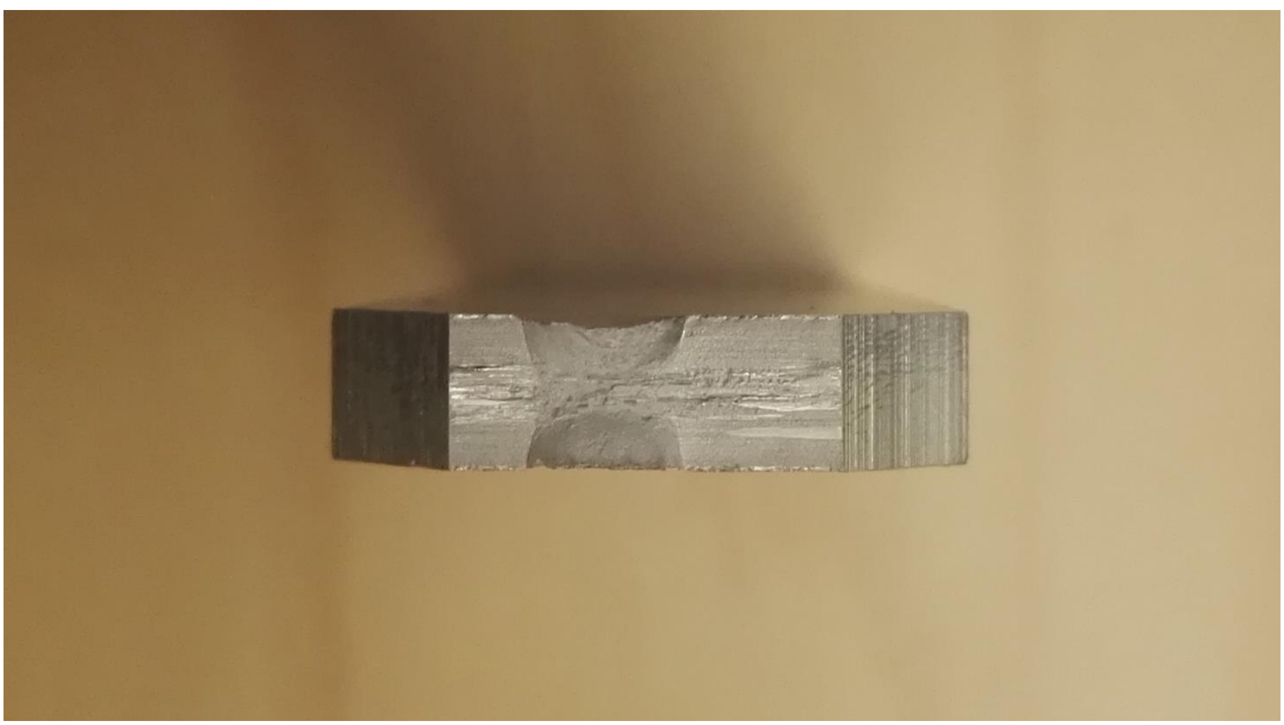

FIGURE 10 SPECIMEN 13, MAX LOAD 120 MPA, FATIGUE LIFE 116732 CYCLES, R=0.5

2. Difference between Elastic and Plastic Model

The aim of this paragraph is to estimate the error committed in considering an elastic model instead of a plastic one while studying a V-sharp notch and computing SED.

The figure below shows the true stress strain curves of 6082-T6 aluminum alloy. The flow stress increased rapidly as the strain increased. When the stress reached a certain point, the material began to yield. After entering the plastic stage, under the effects of work-hardening and dynamic recovery, flow stress increased much slower than the beginning part. When the stress reached a certain value, the material began necking and local stress increased sharply (2).

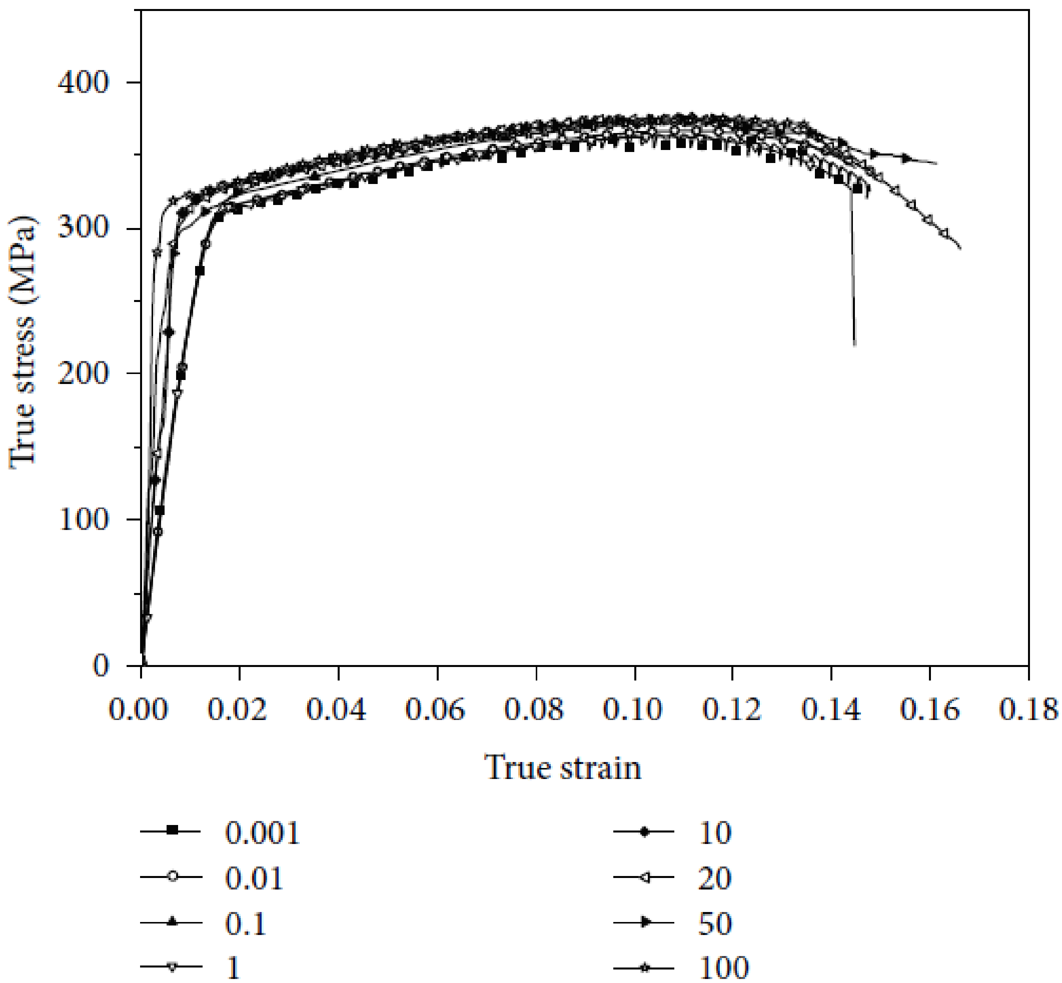

FIGURE 11 TRUE STRESS-STRAIN CURVE OF ALUMINUM ALLOY 6082-T6 (2)

This is the curve implemented in Ansys to compute the plastic model, from different value of the strain rate the material shows different value of the UTS and the yield stress.

Since the material showed no significant yield point, therefore the strain of 0.2% was used as the yield point. As the strain rate increased from 0.001s−1 to 100 s−1, the yield stress increased from 306.1 MPa to 322.63 MPa, increased by 5.4%, and the tensile strength increased from 364 MPa to 384 MPa, increased by 5.49% (2). So an average value have been used, a yield stress of 315 MPa. The plastic part of the plot has been modelled using Johnson Cook law:

$$\sigma = A + B\epsilon_p^n$$

By fitting the experimental data the value of the constants are achieved (2):

$$A = 305.72$$

$$B = 304.9$$

$$n = 0.6796$$

The curve is plotted until a strain of 1, this is obviously absurd, but it is necessary to avoid errors near the notch tip, where the strain might be high for high value of the stress.

The mesh used is refine, even with SED, because the following is a plastic model, which needs to be studied with more precision than the elastic one. It is shown that a more precise model allows to obtain a better solution, but it is more complicated to compute.

Through Ansys it is possible to plot the equivalent stress and strain. In the following figures this plot is shown for a load of 120 MPa and 40 MPa and looking at the superior limit of the scale it is possible to notice that a plastic model shows higher strains than the elastic one, but the stress is obviously less because the materials yields.

All the plots are shown with the same mesh.

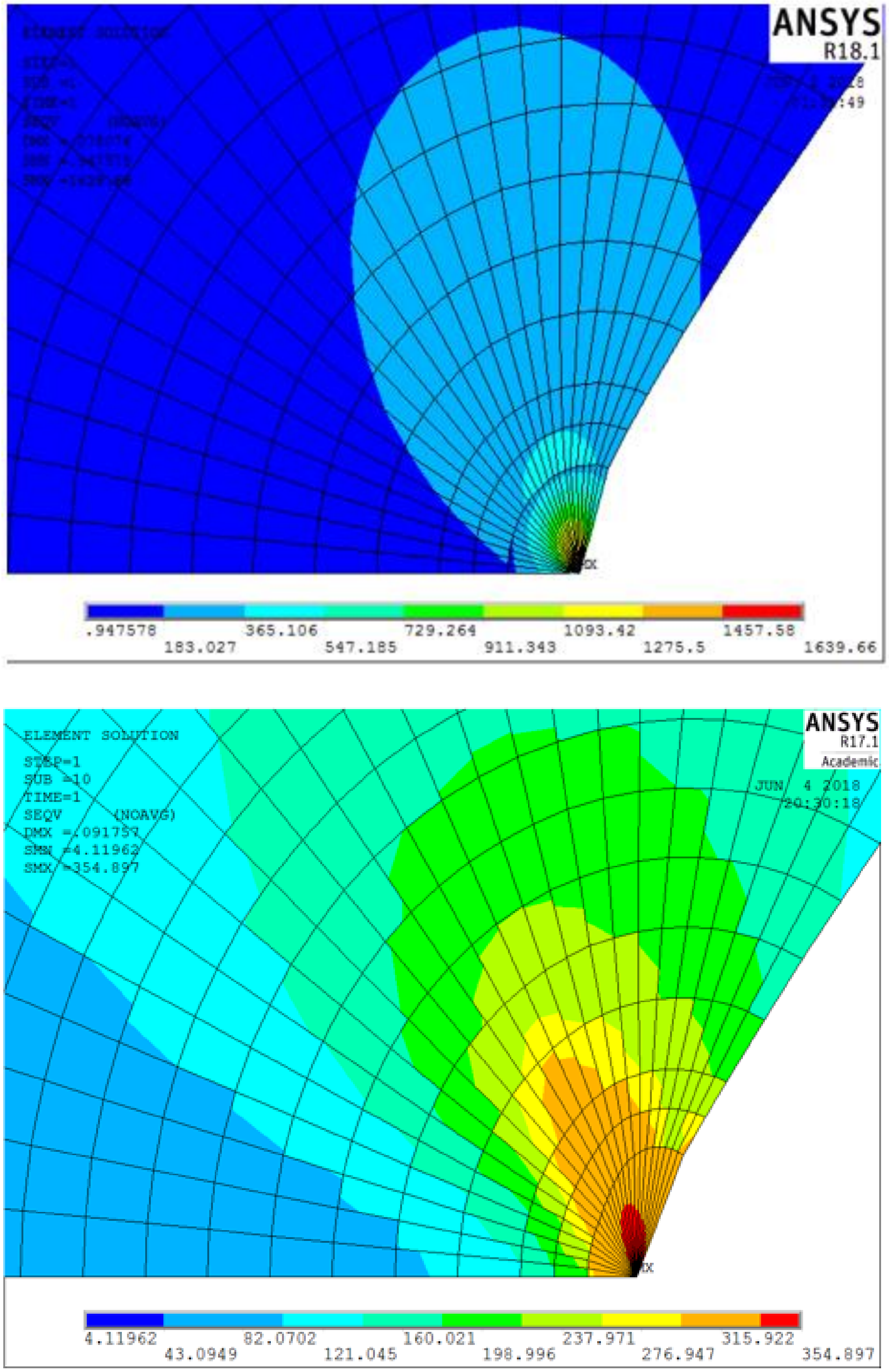

FIGURE 12 EQUIVALENT STRESS IN THE ELASTIC AND PLASTIC MODEL (120 MPA)

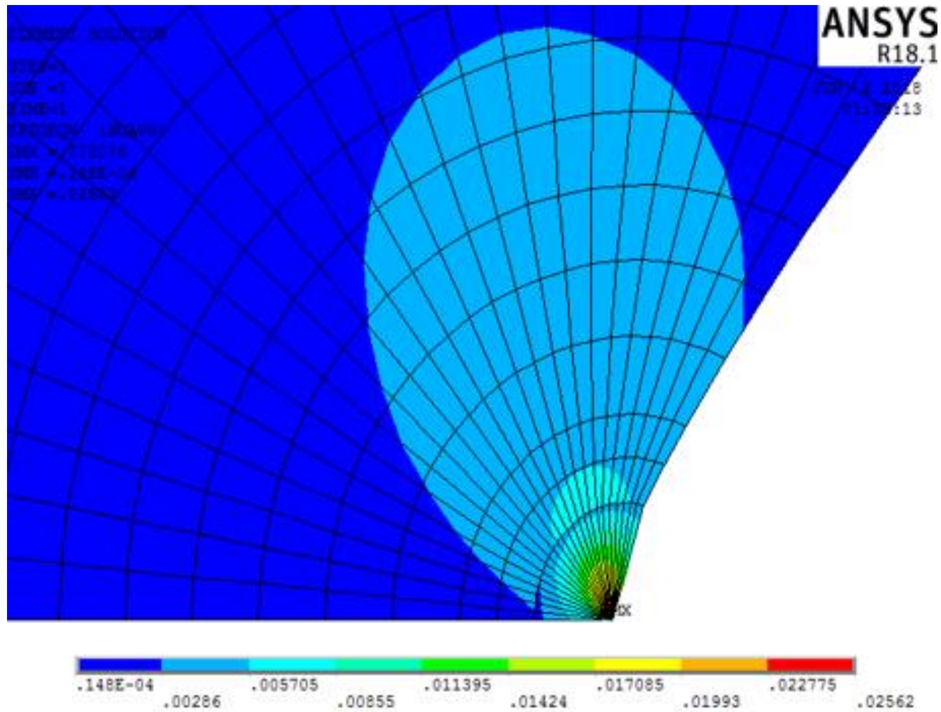

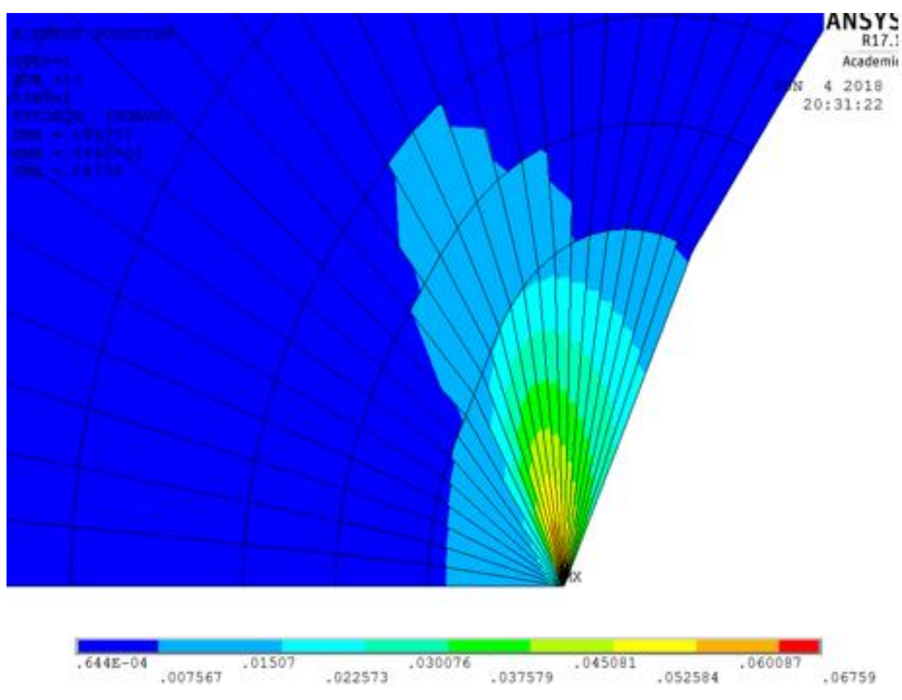

FIGURE 13 EQUIVALENT STRAIN IN THE ELASTIC AND PLASTIC MODEL (120 MPA)

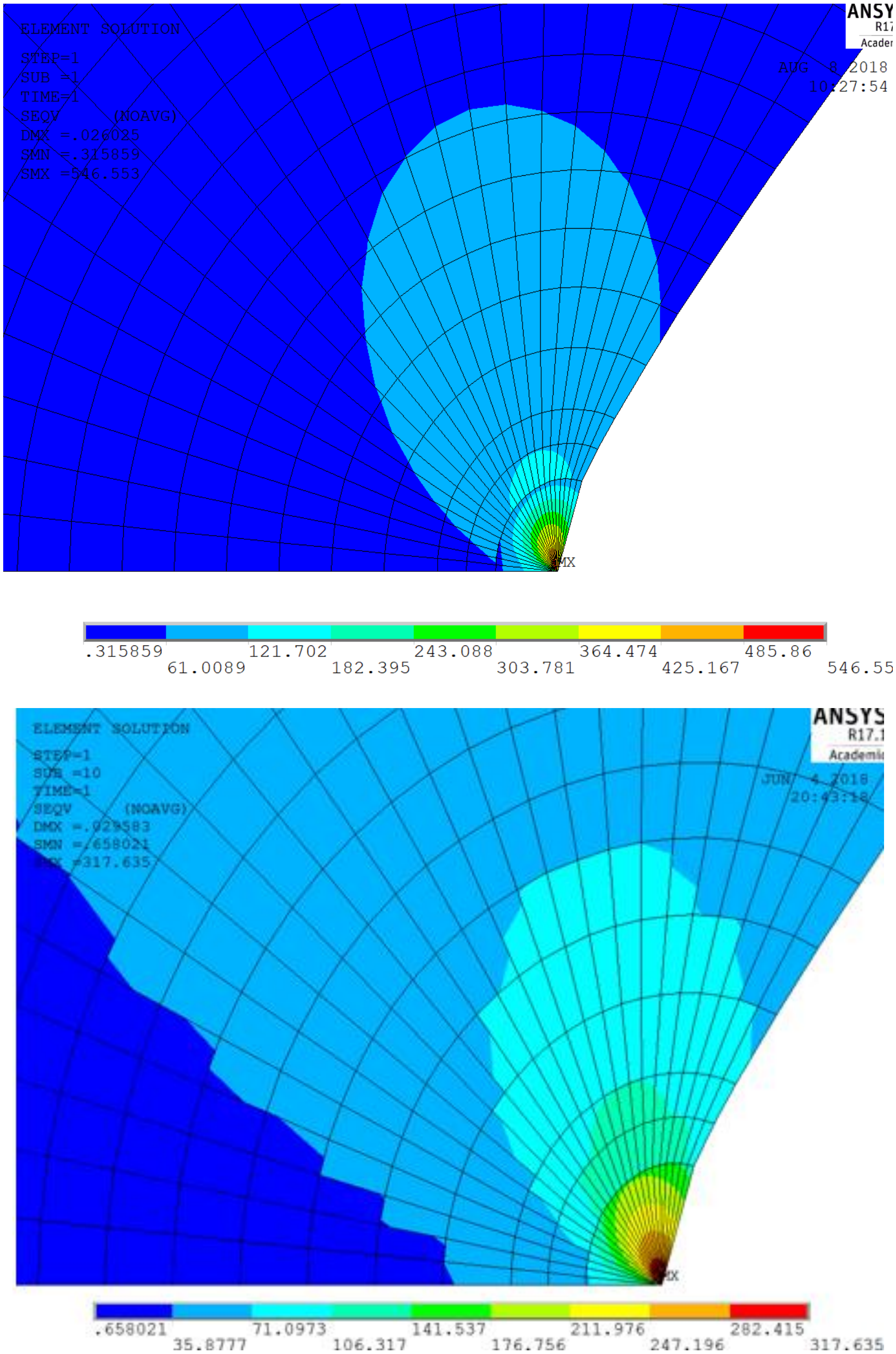

FIGURE 14 EQUIVALENT STRESS IN THE ELASTIC AND PLASTIC MODEL (40 MPA)

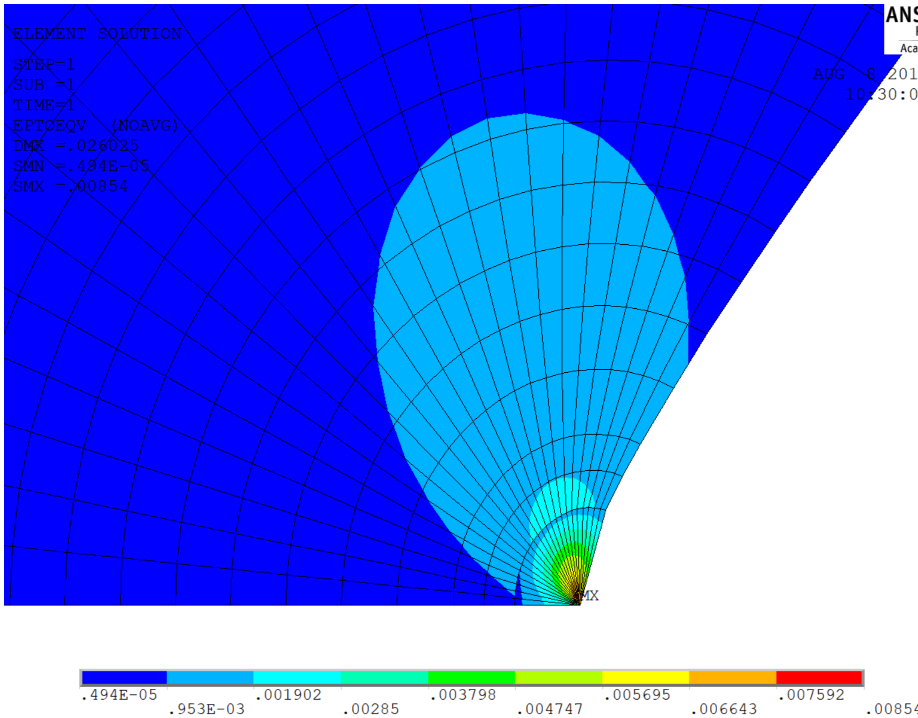

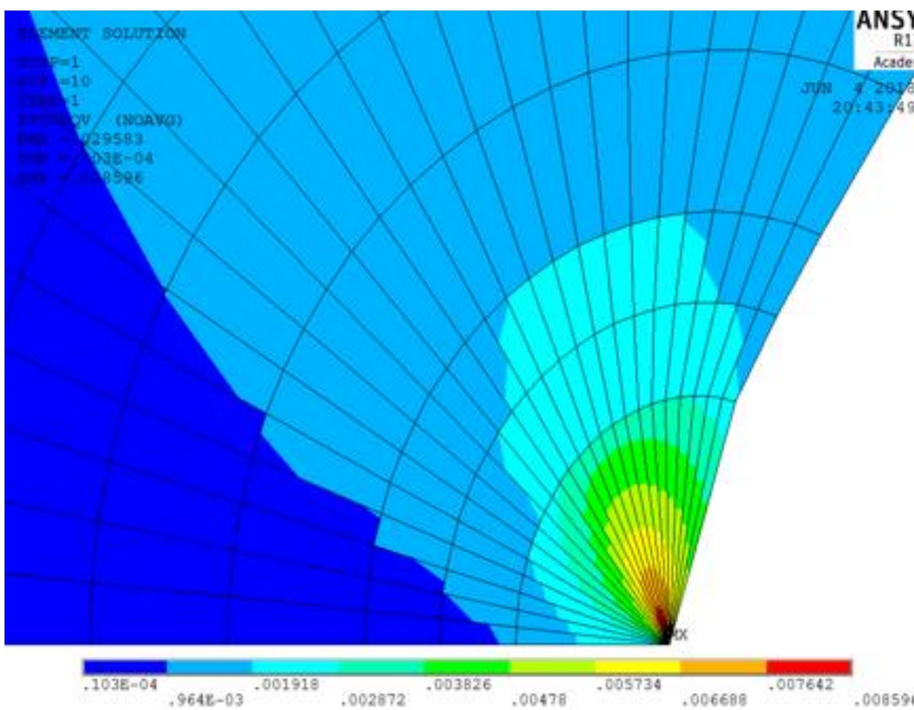

FIGURE 15 EQUIVALENT STRAIN IN THE ELASTIC AND PLASTIC MODEL (40 MPA)

If the load is high the difference of SED between the elastic and the plastic model is higher because the plastic region is bigger, in fact, for the highest load at which the specimens are loaded the difference is the 28%, which is anyway an acceptable error for the model used, while when the specimen is less loaded the difference is even less.

Stress [MPa]	**Sene [Nmm]**	**Volu [mm3]**	W_{pl} **[Nmm/mm3]**	W_{el} **[Nmm/mm3]**	**error**
120	0,035	0,017	2,038	1,465	28 %
40	0,003	0,017	0,186	0,163	12 %

The following plot is an output of Ansys and shows how the stress increases in time in the plastic model in a node close to the notch tip when the load is 120 MPa. It can be plotted using Time Hist Postpro, between the first and the second circumference closest to the notch tip with the finest mesh possible using the command kscon. It is clear that with a plastic model, the material yield and the stress reaches a plateau at 315 MPa.

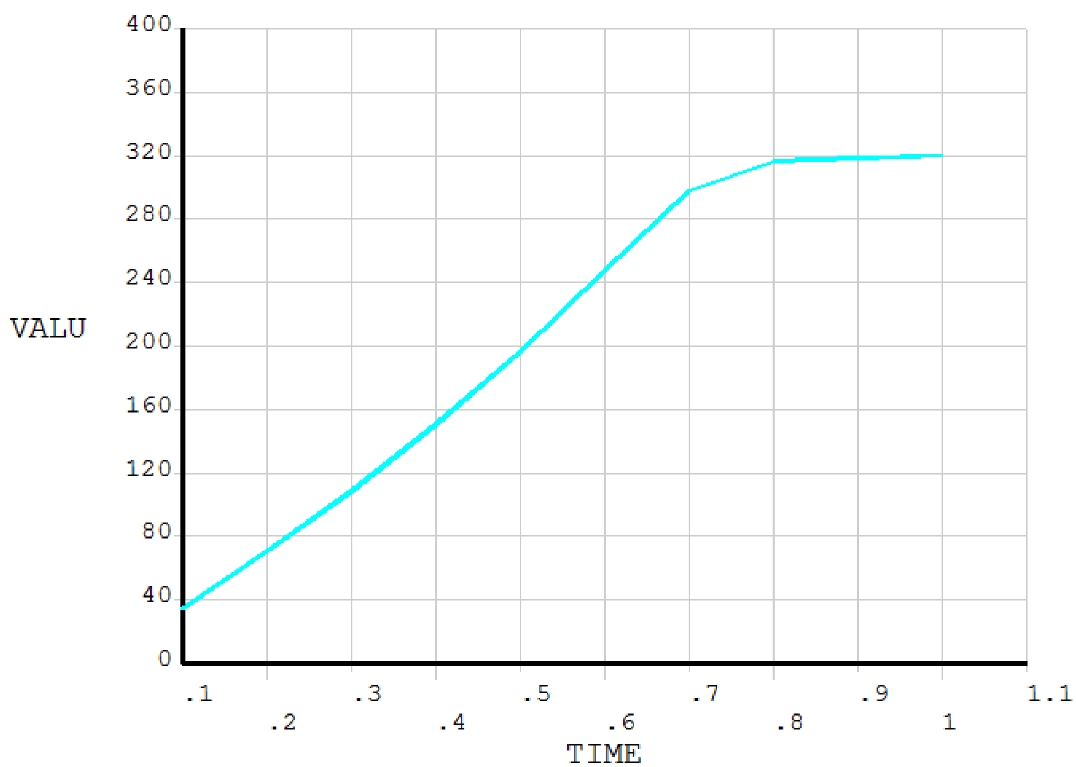

FIGURE 16 STRESS VS TIME IN A NODE CLOSE TO THE NOTCH TIP

Time is equal to one when all the sub steps are completed. A convergence study is made to choose the correct number of sub steps. For a load of 40 MPa 10 of them are enough as shown in the plot below

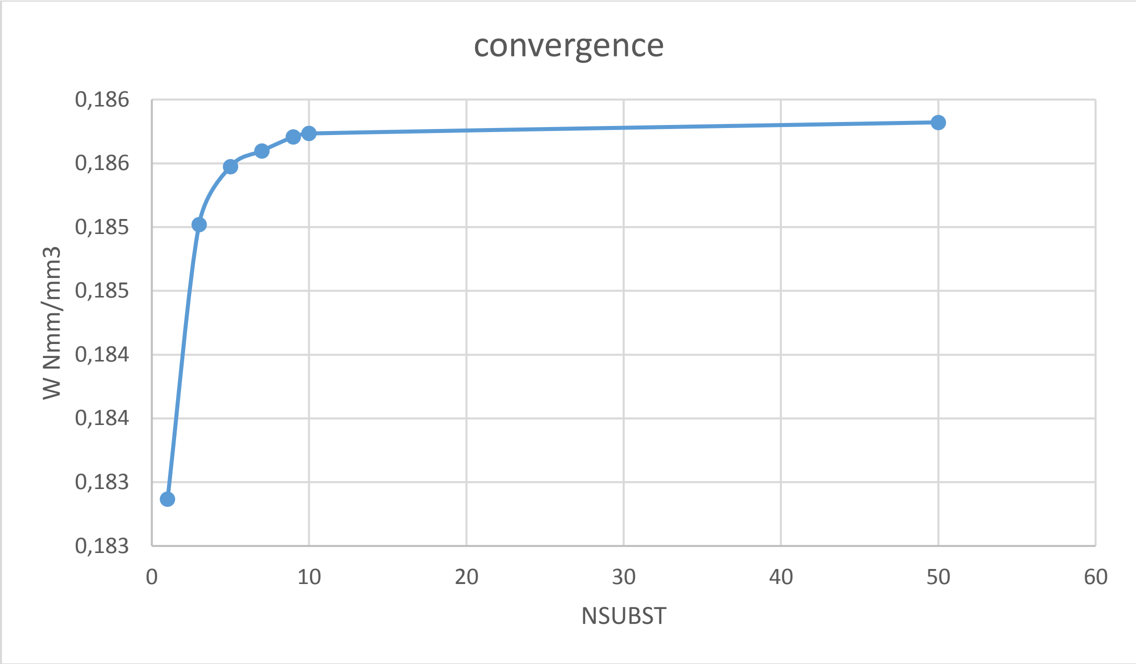

FIGURE 17 CONVERGENCE STUDY

10 subset are thus chosen for all the computations.

3. Computation of the Notch Stress Intensity Factor

As explained in the initial review the N-SIF cannot be used to draw the Wöhler curve when the geometry changes because its unit depends on an exponent which varies with the V-notch angle.

This problem has been overcome by using the mean value of the strain energy density range present in a control volume of radius R_c surrounding the area near the stress concentration.

Once SED is known, the N-SIF can though be calculated, through the following expression (3):

$$K_1^N = (R^*)^{1-\lambda_1}\sqrt{\frac{E\,\bar{W}}{e_1}}$$

R^* has here been assumed to be equal to R_0, the critical radius of the material.

The values of λ_1 and e_1 for an opening angle of 90^o can be found in literature

The notch stress intensity factor has been computed both using SED and stresses and the results are compared, showing that SED method is very precise even though less elements are required in the FEM model.

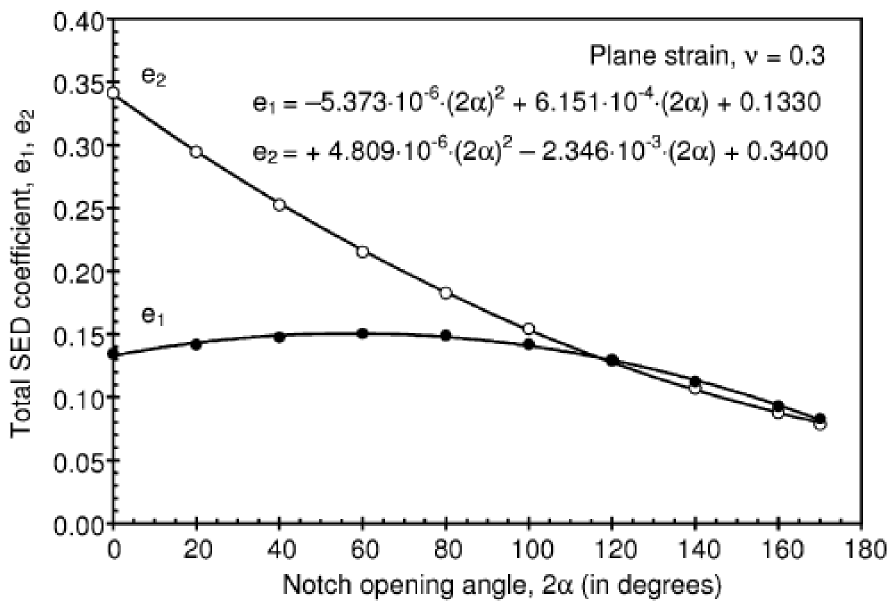

FIGURE 18 SHAPE FUNCTIONS ϵ_1 AND ϵ_2 VERSUS THE NOTCH OPENING ANGLE (3)

2α (rad/π)	q	r_0/ρ	Mode I λ_1	χ_1	μ_1	Mode II λ_2	χ_2	μ_2
0	2.000	0.500	0.500	1.000	−0.500	0.500	1.000	−0.500
1/6	1.833	0.455	0.501	1.071	−0.424	0.598	0.921	−0.259
1/4	1.750	0.429	0.505	1.166	−0.389	0.660	0.814	−0.145
1/3	1.667	0.400	0.512	1.312	−0.354	0.731	0.658	−0.033
1/2	1.500	0.333	0.544	1.841	−0.280	0.909	0.219	0.190
3/4	1.250	0.200	0.674	4.153	−0.150	1.302	−0.569	0.553

It is possible to compute K_I with the following expression, using stresses (3)

$$K_{\mathrm{I}} = \lim_{r\to 0} \sqrt{2\pi r}\,\sigma$$

In which r is the distance from the notched tip and σ is the stress applied.

As it was expected the stress rise to a singularity at the pointed crack tip, while, in a radius close to the notch tip, the N-SIFs calculated express a plateau, which is a good estimate of the N-SIFs.

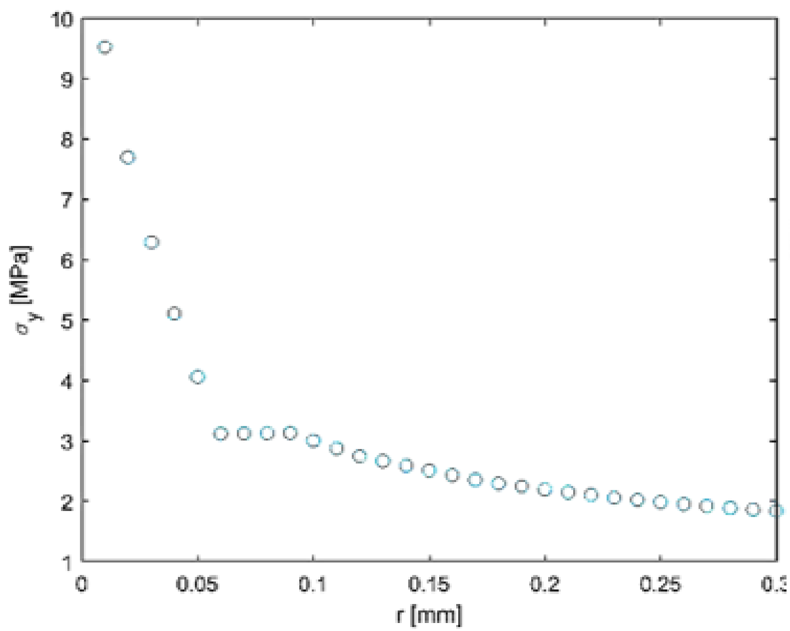

FIGURE 19 PLOT OF STRESS IN FUNCTION OF THE DISTANCE FROM THE TIP

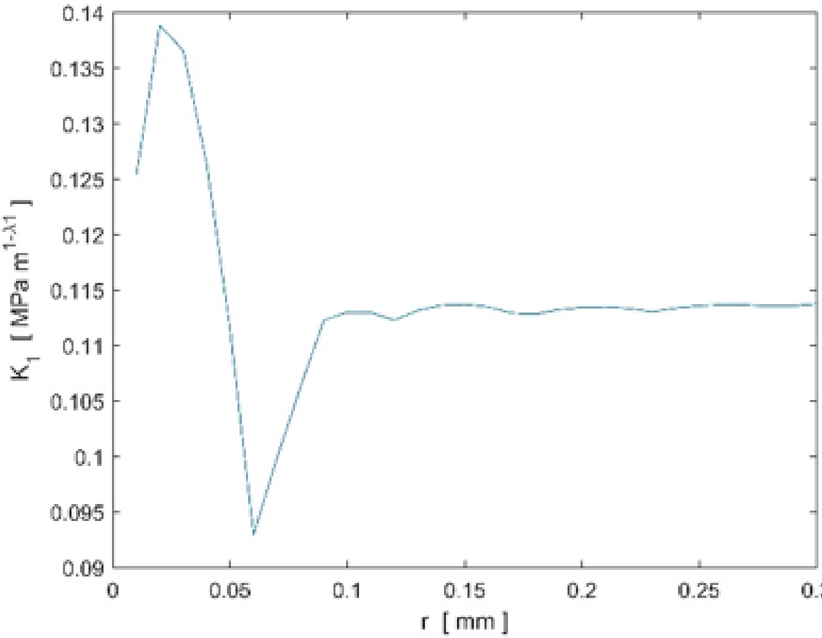

FIGURE 20 PLOT OF NSIF IN FUNCTION OF THE DISTANCE FROM THE TIP

Stresses obtained at a node belonging to faced finite elements are very different when a coarse mesh is used. As a natural consequence, the degree of mesh refinement required for the accurate determination of the strain energy is much lower than that required for the stress fields, simply because in the former case no derivation or integration process is really involved (4).

In fact, the mesh used to compute K_1 through stresses is more refined that the one used with SED, as shown in the following figure

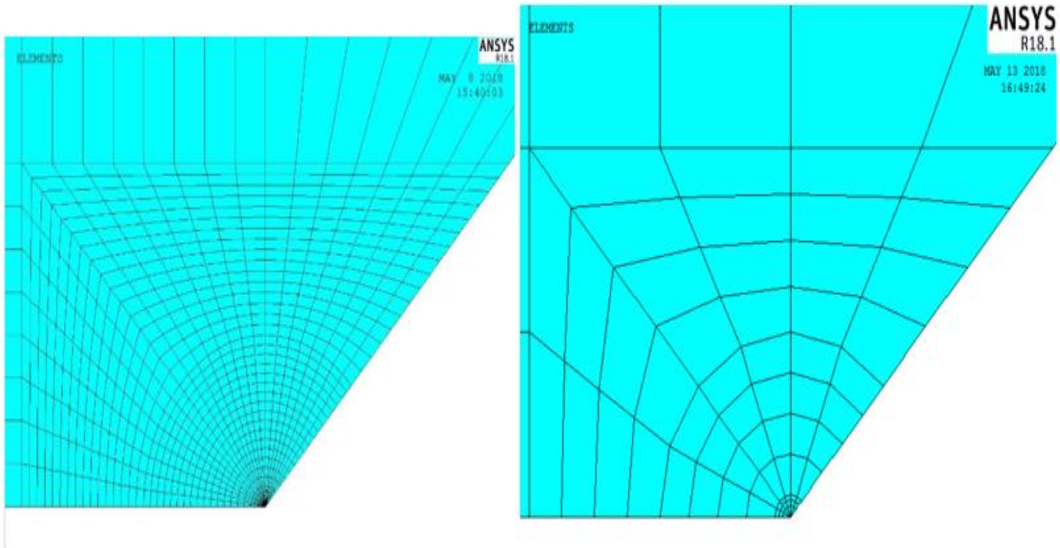

FIGURE 21 COMPARISON BETWEEN REFINE AND COARSE MESH

The values of K_1 computed are very similar as it is shown in the table below

K_1 [MPa mm$^{1-\lambda_1}$]		
stress	SED	difference
0,113	0,109	3,6%

A comparison between plane strain and plane stress has been made to verify that the value of K_1 is lower in conditions of plane stress.

K_1 [MPa mm$^{1-\lambda_1}$]		
Plane Stress	Plane Strain	difference
0,101	0,111	9,5%

A comparison has been made by plotting the scatter curve for the welded aluminum and the values of SED calculated for the samples tested.

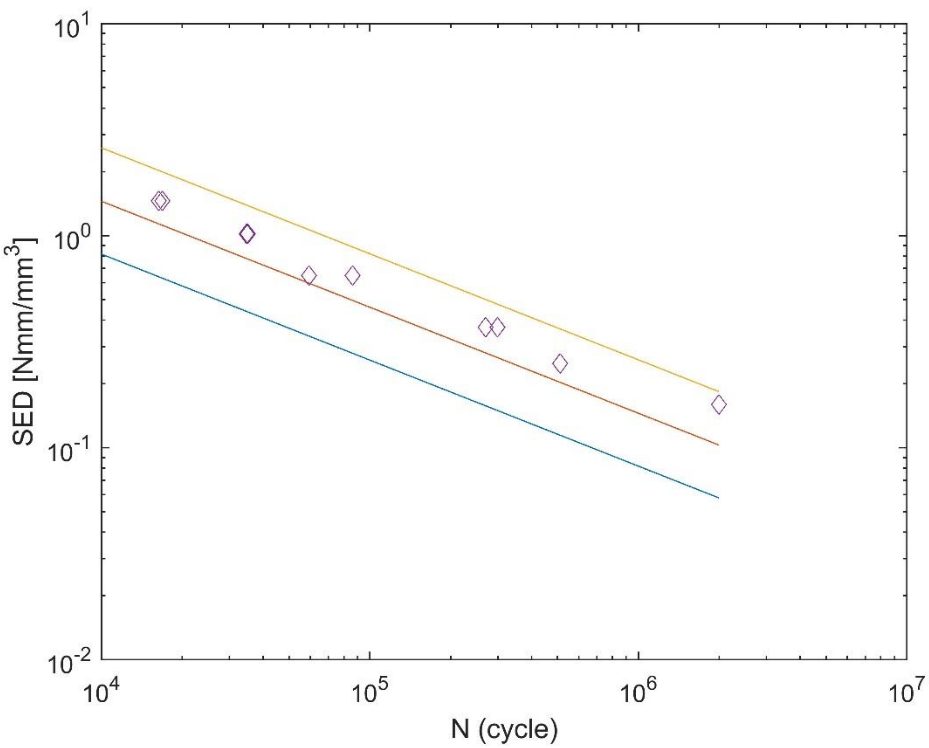

FIGURE 22 DATA FITTING IN WELDED ALUMINUM SCATTER BAND

As expected, the values computed for the samples fit in the welded aluminum scatter curve and they seem to be more resistant than the welded specimens.

4. Dimensionless Parameter Y

The stress intensity factor can be defined as

$$\Delta K = \sigma Y \sqrt{a}$$

In which σ is the stress applied, a is the length of the crack and Y is a dimensionless parameter.

Using a parametric Ansys model and the expression above it is possible to compute the value of Y, while the crack is progressing.

The aim is to find an expression for Y, suitable for V-shape notches, with an opening angle of 90^o, in function of the ratio between the crack's length and the width of the sample.

When the SED is known it is possible to calculate K_1 by the well-known expression

$$K_1 = R_0^{1-\lambda_1} \sqrt{\frac{EW}{e_1}}$$

In which λ_1 and e_1 must be computed for an angle of 0^o

A fourth-grade polynomial can fit the values obtained

$$Y\left(\frac{a}{W}\right) = 5852\left(\frac{a}{W}\right)^4 - 7647\left(\frac{a}{W}\right)^3 + 3712\left(\frac{a}{W}\right)^2 - 788.5\left(\frac{a}{W}\right) + 63.67$$

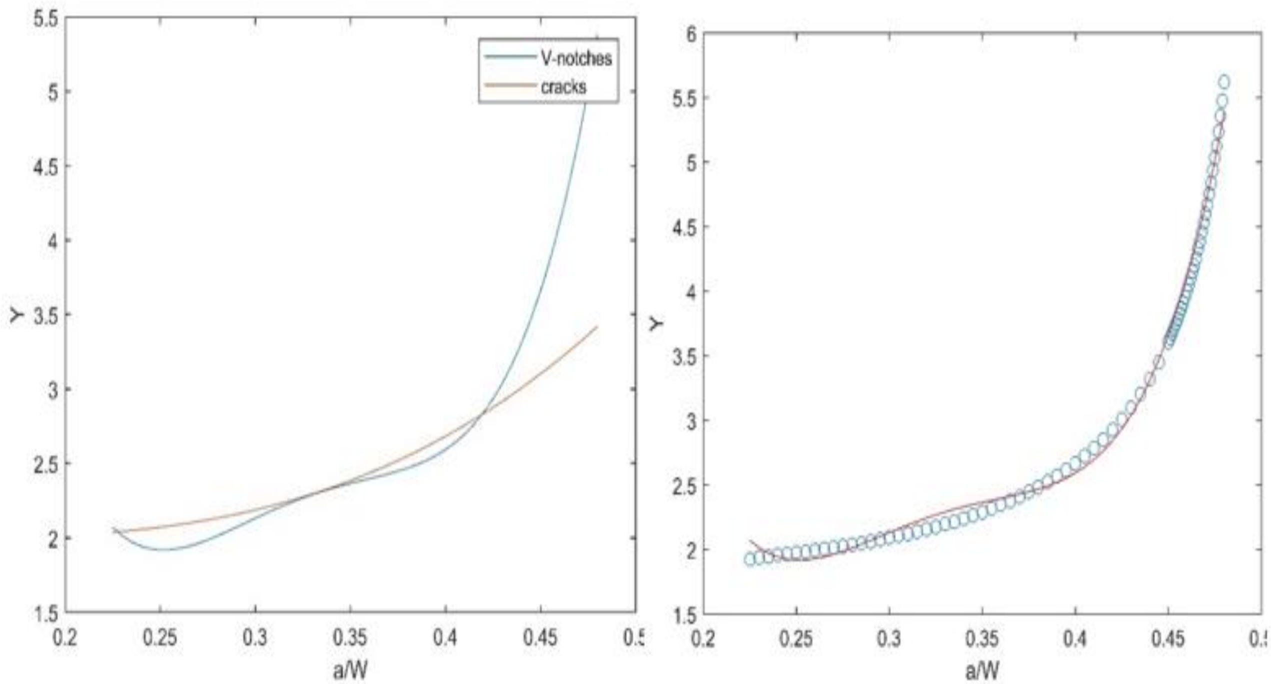

FIGURE 23 COMPARISON BETWEEN V-NOTCH AND CRACK AND DATA FITTING FOR V-NOTCH

This expression seems to be quite close to that used for double crack for low value of a, while the two curves tend to spread for high value of the crack's length.

5. Initiation and Propagation of the Crack

It is known from the paper written by Paris and Erdogan in 1963 (5) that by plotting on a log-log diagram the value of the derivative of the crack length with respect to of the number of cycles in function of the SIF, the data can be quite well fitted by a straight line, so the following expression can be written

$$\frac{da}{dN} = C\Delta K^{n}$$

Where C and n are two parameters which depend on the material and the load ratio.

The aim of this paper is to find a value of the coefficient C and n of the Paris' law, adapted for the Strain Energy Density.

$$\frac{da}{dN} = C'\Delta W^{n'}$$

In the case of non-singular mode II and considering a null opening angle of the notch it is possible to determine the mode I N-SIF a posteriori from SED, through the following expression

$$K_I = \sqrt{\frac{R_0 E W}{e_1}}$$

After some easy computation the parameters of interest and the number of cycles can be expressed in the following way

$$C' = C\left(\frac{R_0 E}{e_1}\right)^{n/2}$$

$$n' = n/2$$

$$N_p = \int_{a_0}^{a_f} \frac{da}{C' W^{n'}}$$

W is a function of the length of the crack and can be found by fitting the different value of W while the crack is propagating. It is possible to compute an Ansys parametric model in which the stress at the restricted area σ_1 is equal to 1 MPa and find the function $W_1(a)$, expressed by an exponential function

$$W_1(a) = A\exp(B\ a) + C\exp(D\ a)$$

In which $A = 3.223E - 5$; $B = 0.2868$; $C = 1.858E - 14$; $D = 2.608$

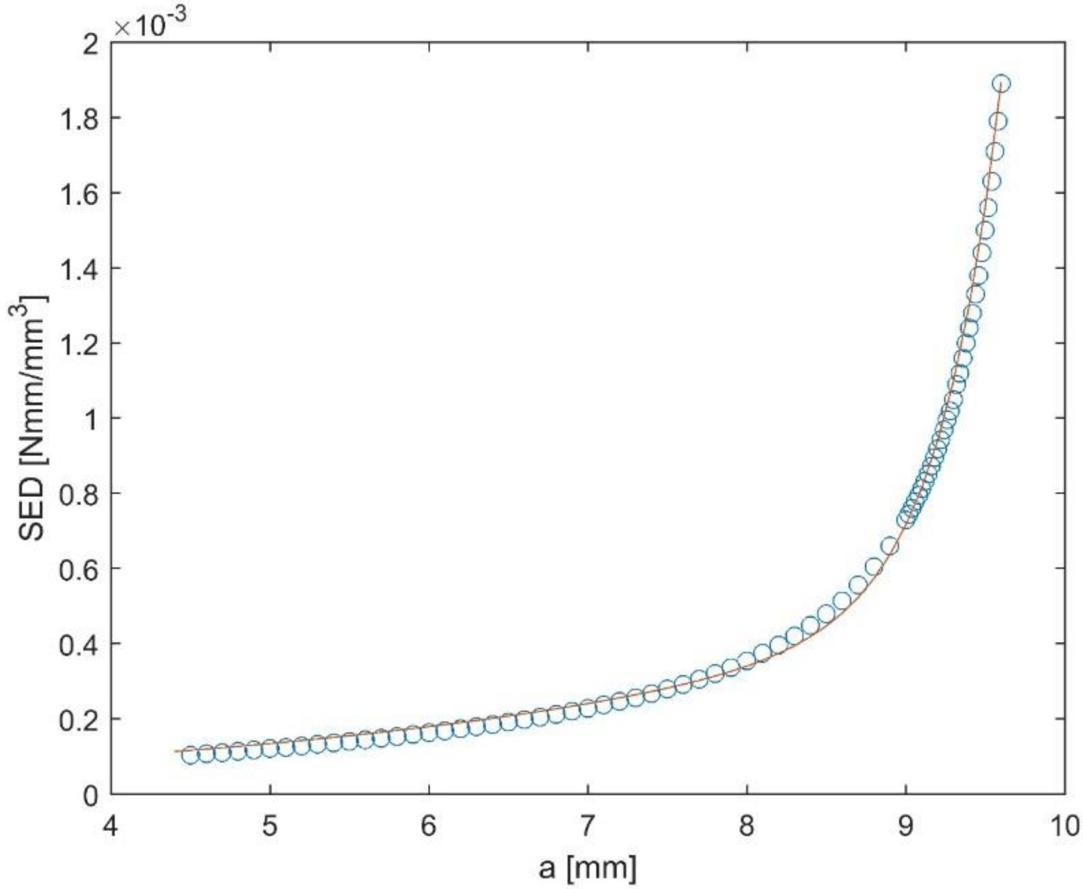

FIGURE 24 SED IN FUNCTION OF THE LENGTH OF THE CRACK

To find the function $W(a)$ for each specimen the following expression can be used

$$W(a) = W_1(a) \cdot \sigma^2$$

In which σ is the value of stress at the restricted area.

Finally, the number of cycles between the initiation of the crack and the failure of the specimen is

$$N_p = \frac{1}{C'\sigma^{2n'}} \int_{a_0}^{a_f} \frac{da}{W_1(a)^{n'}}$$

Where a_f has been measured from the crack surface.

The integral can be numerically solved using the '*integral'* function in matlab and considering that the value of the Paris' parameters for the aluminum alloy 6082-T6 are present in literature (6). Also the number of cycles necessary to initiate the crack can be computed

$$C' = 6.1154e - 05$$

$$n' = 1.3235$$

$$N_i = N_f - N_p$$

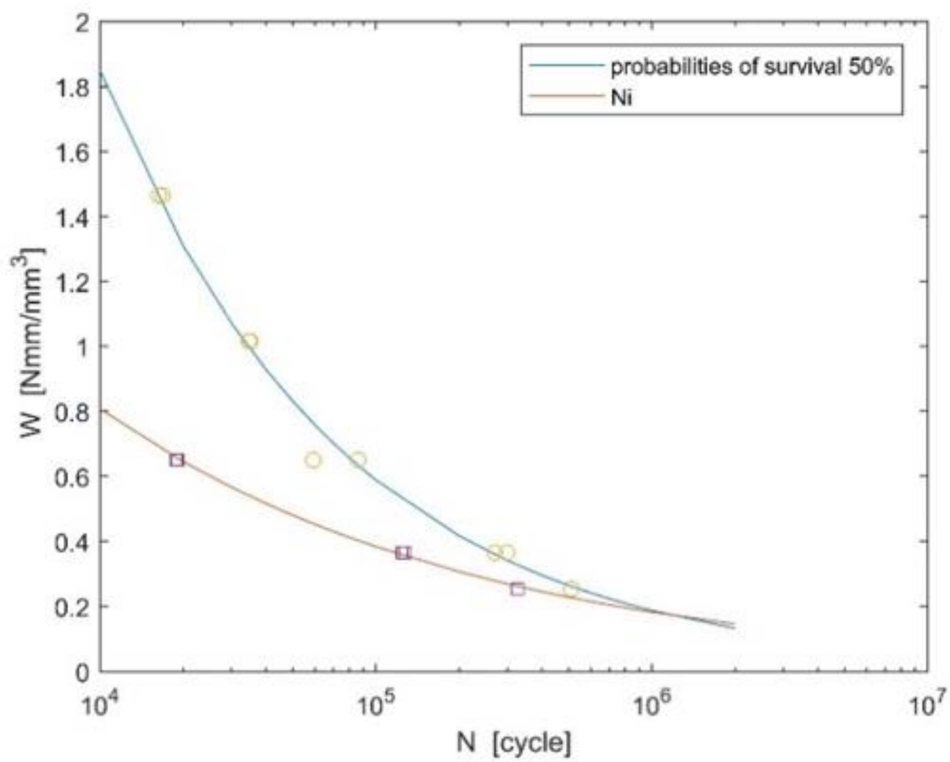

FIGURE 25 SED IN FUNCTION OF THE NUMBER OF CYCLES IN SEMI-LOG PLOT

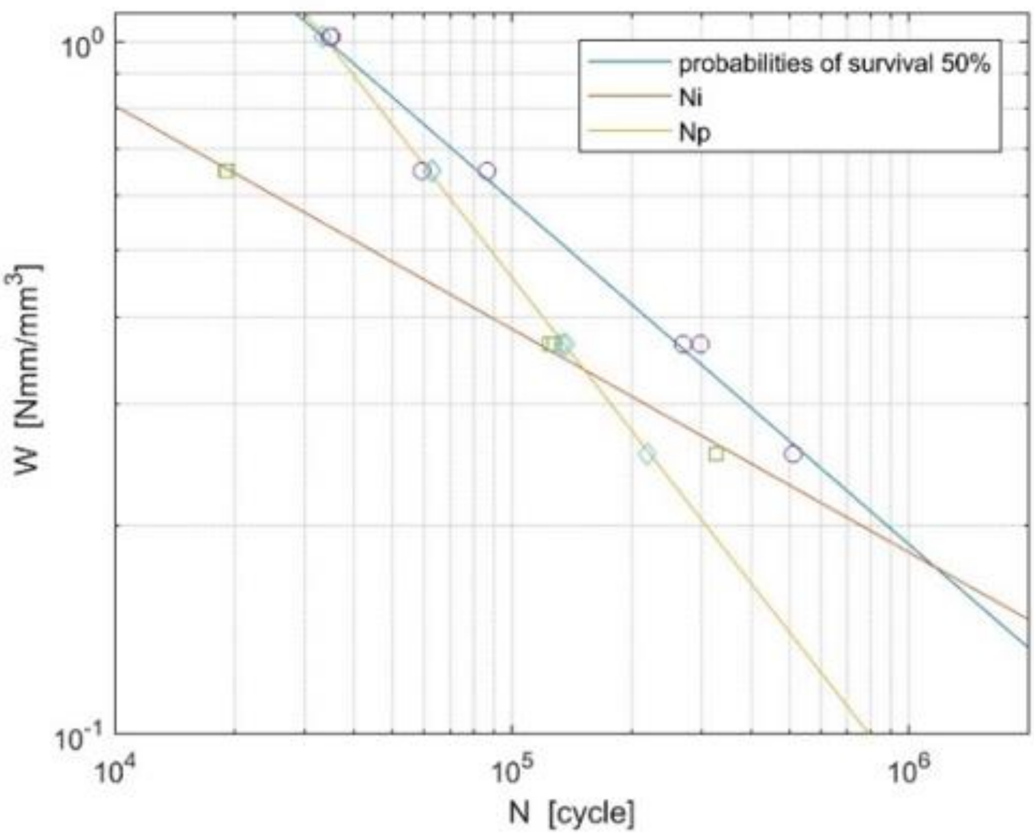

FIGURE 26 SED IN FUNCTION OF THE NUMBER OF CYCLES IN LOG-LOG PLOT

From the figures it is clear that at low cycles the propagation is prevalent, while at high cycle the initiation is so. For very low cycle the Np exceeded the whole life of the specimen and this is clearly a mistake due to the approximations made. This model gives good result in a range between 3·E04 and 1·E06 cycles and outside this range the Np, computed using the Paris' law is different from its actual value. Another relevant observation is that the shift from a life of the specimen dominated by the propagation of the crack to that dominated by the initiation occurs between 1·E05 and 2·E05 cycles, this is due to the fact that the specimen has a sharp notch, so the crack initiates earlier than in an un-notched one.

No experiments were made to compute the parameters *C* and *n* and they are taken from literature, for this reason the focus of this chapter is the analytical part, useful to find equivalent parameters and to apply Paris law to SED, even though the results seems to be consistent.

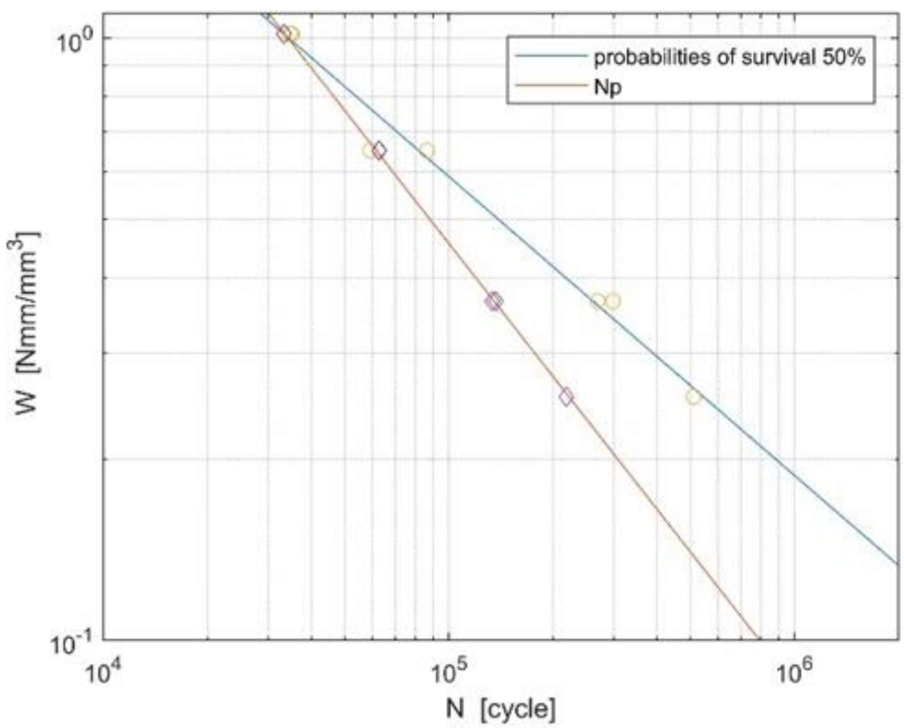

FIGURE 27 INFLUENCE OF SED ON THE PROPAGATION OF THE CRACK

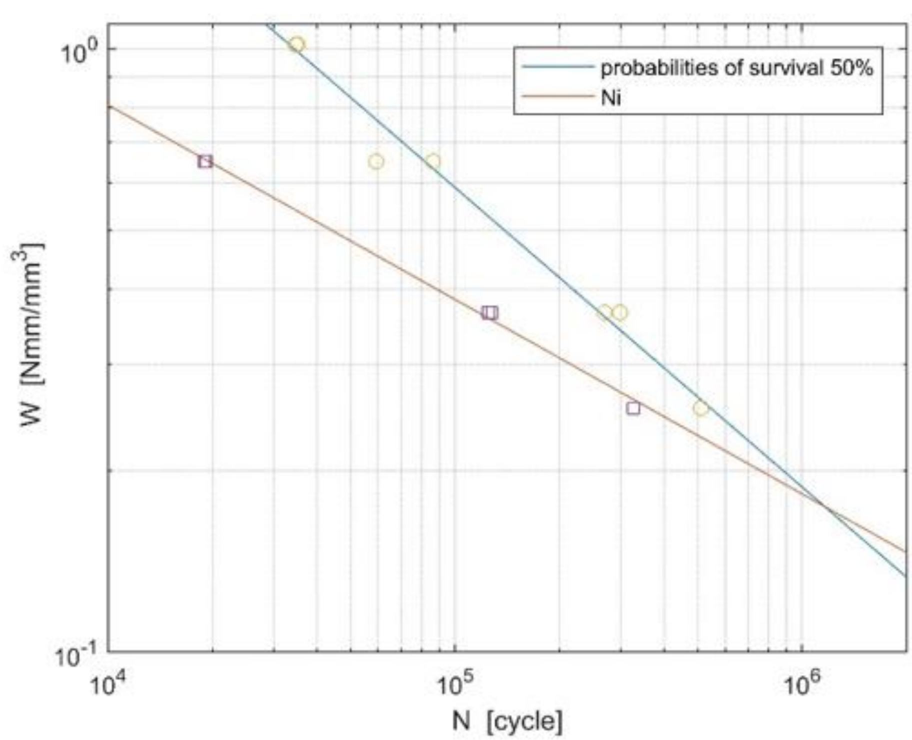

FIGURE 28 INFLUENCE OF SED ON THE INITIATION OF THE CRACK

6. Haigh Diagram

Both the data from the specimens loaded with R=0 and R=0.5 are used to plot the Haigh diagram using SED formulation. The coordinates of each point belonging to the plot are mean SED, alternative SED and number of cycles to failure. This plot has been projected on the W_m, W_a plane.

The SED components cannot be computed in a similar way to that used for the stress ones:

$$W_{max} = W_1 \cdot \sigma_{max}^2$$

$$W_{min} = W_1 \cdot \sigma_{min}^2$$

$$W_a = \frac{W_{max} - W_{min}}{2}$$

$$W_m = \frac{W_{max} + W_{min}}{2}$$

As explained in the Chapter dedicated to the Paris method, integrated with SED, W_1 is the value of SED, when the specimen is loaded with a stress of $1\ MPa$ at the restricted area.

Using these definitions both the Wöhler and Haigh plot are nonsense, because it seems that when the load ratio increases the material can resist to a higher W_a as it is shown in the following plot

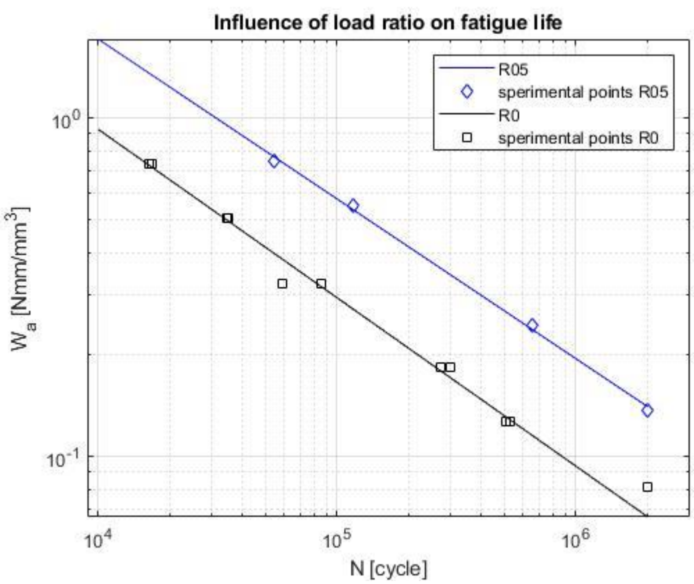

FIGURE 29 ERRONEOUS WÖHLER DIAGRAM

To avoid such problems, it is necessary to define new variables which are not the actual values of the mean and alternative components of SED, bot allows to plot a meaningful Haigh plot:

$$W'_m = W_1 \sigma_m^2$$

$$W'_a = W_1 \sigma_a^2$$

Knowing that:

$$\sigma_a = \frac{\sigma_{max} - \sigma_{min}}{2}$$

$$\sigma_m = \frac{\sigma_{max} + \sigma_{min}}{2}$$

Consequently for R=0.5

$$W'_m = 9 \cdot W'_a$$

It is now necessary to find a point correspondent to the σ_{uts} in the Haigh diagram plotted with SED, through which it is possible to draw the iso number of cycles lines, using the Gerber relation.

This value has been computed by doing the mean of the value of SED at the fracturing point for all the specimen loaded with a null load ratio.

Knowing that the value of SED for a load of 1 MPa in function of the length of the crack is

$$W_1(a) = A \cdot \exp(B \cdot a) + C \cdot \exp(D \cdot a)$$

In which $A = 3.223E - 5$; $B = 0.2868$; $C = 1.858E - 14$; $D = 2.608$

It is necessary to measure the length of the crack on the fractured surface to compute the value of SED. This procedure is made for all the samples loaded with R=0 and the mean value of SED right before the rupture of the specimen is 3.41 $N \cdot mm/mm^3$.

specimen	af[mm]	W1(af) [Nmm/mm3]	Wf [Nmm/mm3]
2	8,08	3,53E-04	5,09
11	7,92	3,30E-04	4,75
6	8	3,70E-04	3,70
8	8,18	3,71E-04	3,71
3	8,78	5,63E-04	3,61
9	9	6,14E-04	3,93
5	8,68	5,15E-04	1,85
10	9,385	1,27E-03	4,56
16	8,63	4,94E-04	1,23
12	8,94	6,67E-04	1,67
			3,41

It can be noticed that the size of the final crack at fracture depends on the stress level. The higher stress levels have shorter critical crack sizes and the lower stress levels have larger critical crack sizes.

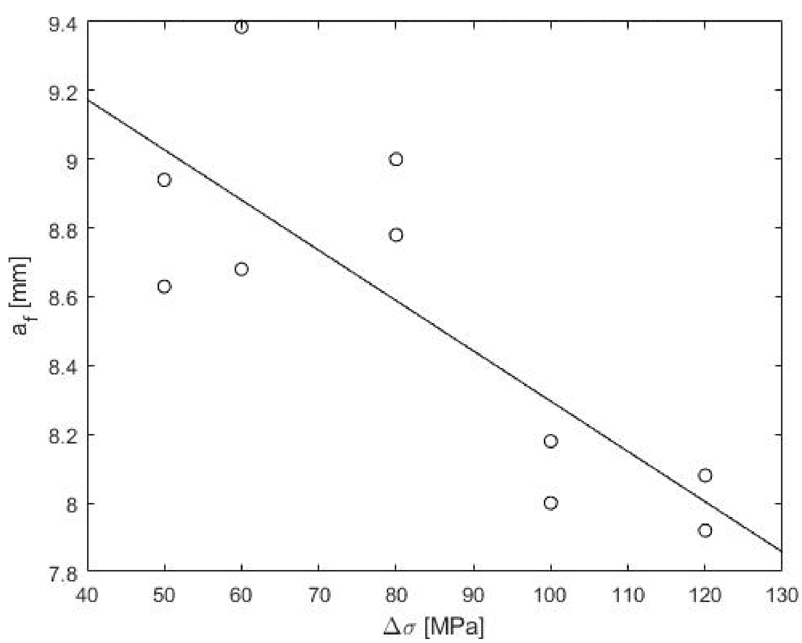

FIGURE 30 VARIABILITY OF THE FINAL LENGTH OF THE CRACK IN FUNCTION OF THE STRESS APPLIED FOR R=0

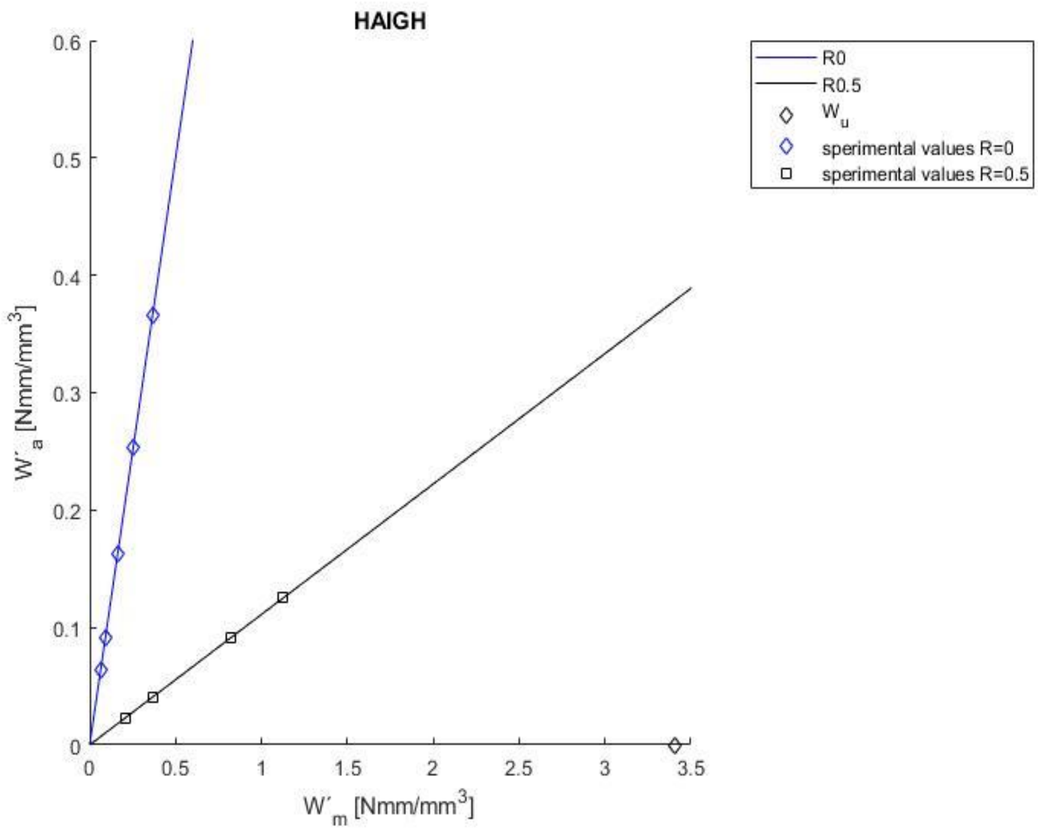

FIGURE 31 EXPERIMENTAL VALUES IN THE HAIGH DIAGRAM

In order to model the effect of the mean stresses, a multitude of formulations have been proposed, most of which use the engineering tensile stress σ_{uts} or the monotonic yield stress σ_y as one of the parameters.

In general, these formulas come from empirical approaches to correlate groups of tests on particular materials. In the literature it is widely documented that there is no general empirical law to relate the effect of mean stress on the fatigue limit (7).

The Gerber relation is used in the following diagrams, a parabola, concave downward that passes through the point W_u on the x-axis, interpolates the iso number of cycles point and crosses the y-axis with horizontal tangent.

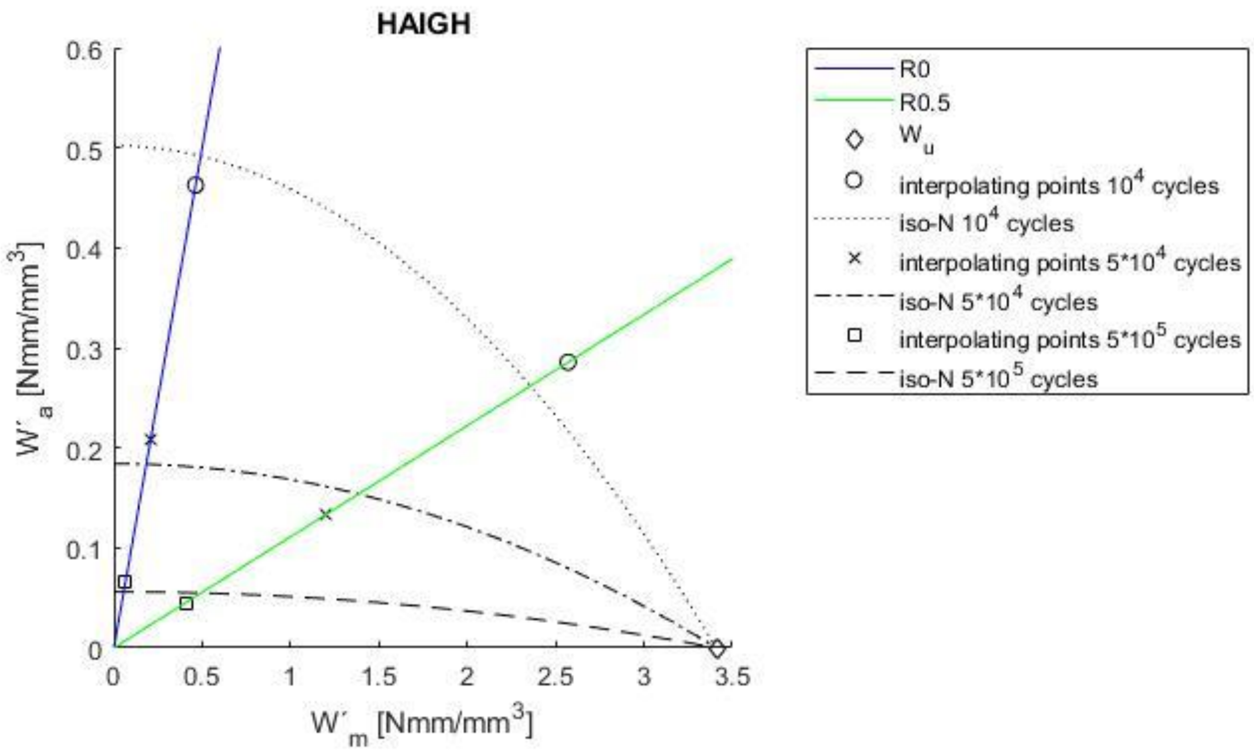

FIGURE 32 GERBER`S RELATION WITH SED

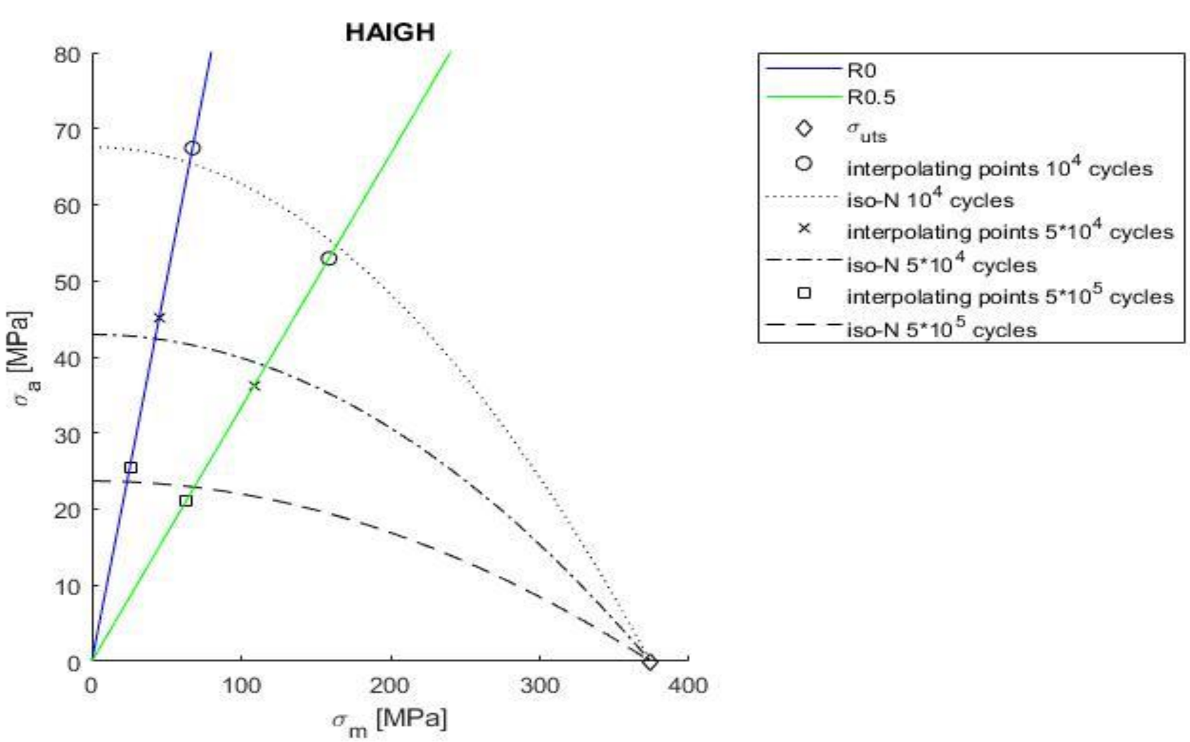

FIGURE 33 GERBER`S RELATION WITH STRESS

The number of cycles at the intersections between the Gerber parabola and the lines at R=0 and R=0.5 are graphically found and the ratio between the predicted life and the experimental one is computed:

Number of cycles computed with SED						
	R0			**R0.5**		
Gerber	1,0E+04	5,0E+04	5,0E+05	1,0E+04	5,0E+04	5,0E+05
Experimental Life	9,0E+03	6,5E+04	7,0E+05	1,2E+04	3,7E+04	3,3E+05
Ratio	1,1	0,8	0,7	0,8	1,4	1,5

Number of cycles computed with stress						
	R0			**R0.5**		
Gerber	1,0E+04	5,0E+04	5,0E+05	1,0E+04	5,0E+04	5,0E+05
Experimental Life	1,1E+04	6,5E+04	7,0E+05	9,0E+03	3,7E+04	3,5E+05
Ratio	0,9	0,8	0,7	1,1	1,4	1,4

The same procedure is adopted with the Goodman relation, represented in the diagrams by a line which passes through point W_u on the x-axis and interpolates the points underlined.

Number of cycles computed with stress						
	R0			**R0.5**		
Goodman	1,0E+04	5,0E+04	5,0E+05	1,0E+04	5,0E+04	5,0E+05
Experimental Life	9,0E+03	5,0E+04	5,6E+05	1,2E+04	5,0E+04	4,3E+05
Ratio	1,1	1,0	0,9	0,8	1,0	1,2

Number of cycles computed with SED						
	R0			**R0.5**		
Goodman	1,0E+04	5,0E+04	5,0E+05	1,0E+04	5,0E+04	5,0E+05
Experimental Life	8,6E+03	5,2E+04	6,0E+05	1,6E+04	4,7E+04	3,6E+05
Ratio	1,2	1,0	0,8	0,6	1,1	1,4

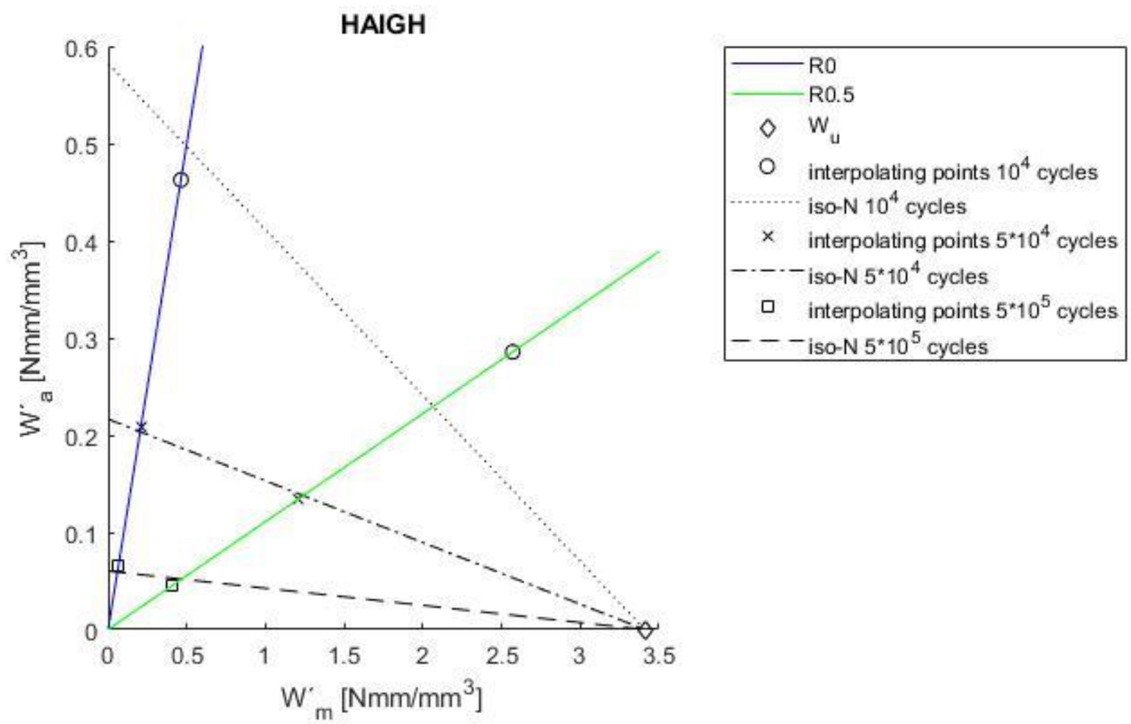

FIGURE 34 GOODMAN`S RELATION WITH SED

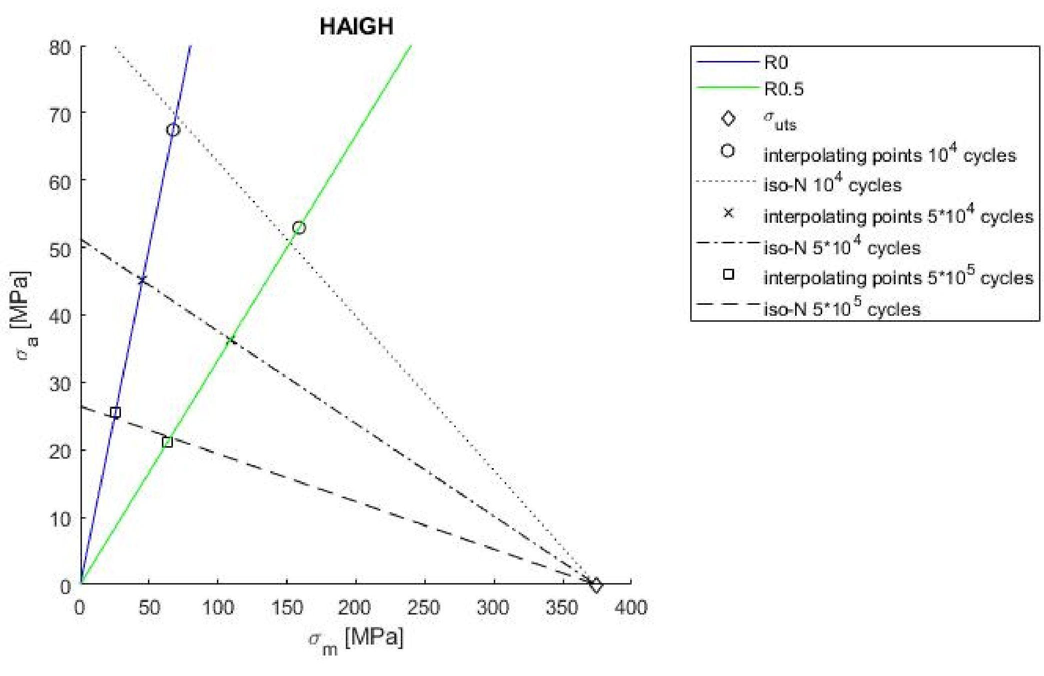

FIGURE 35 GOODMAN`S RELATION WITH STRESS

It is clear that using Gerber relation the precision is very similar using stress or SED, in both cases the critical point is that on the R=0.5 line, because according to Gerber`s relation the specimen should resist 50% and 40% more than it actually does, respectively in SED and stress`s diagram. This level of precision is consistent with that present in the literature (8).

Goodman relation works better with the stress, even though the precision achieved with SED is also acceptable.

It is though possible to use SED method to plot the Haigh diagram, exploiting all the advantages linked to this method, especially for what concern the computation time and the possibility of using coarse meshes, as explained in the dedicated chapter.

7. Equivalent method to characterize the fatigue behavior of the aluminum specimen

The three parameters that characterize a mechanical fatigue behavior are the mean stress, σ_m alternating stress, σ_a and the resulting life, *N*, the application of the data that characterize the mean and alternating stress in one equivalent stress model allows to evaluate theirs effect on the fatigue behavior.

The equivalent value of the stress use in this paragraph is calculated as the fatigue strength, σ_{-1}, when the load ratio R is equal to -1. For example in the Haigh diagram, the iso-N curves, drawn using Goodman`s relation, can be described by the following equation:

$$\sigma_a = \left(-\frac{\sigma_{-1}}{\sigma_{UTS}}\right)\sigma_m + \sigma_{-1}$$

Starting from the experimental data, alternative and mean stress are computed, after that the equivalent stress is computed, both by using Goodman and Gerber models.

$$\sigma_{-1} = \sigma_{Go} = \frac{\sigma_a}{1 - (\frac{\sigma_m}{\sigma_{UTS}})}$$

$$\sigma_{-1} = \sigma_{Ge} = \frac{\sigma_a}{1 - \left(\frac{\sigma_m}{\sigma_{UTS}}\right)^2}$$

The objective of this paragraph is to verify the possibility to apply this method, devised by the researchers of the Department of mechanical Engineering of the University of Brasília (9) to be used with stress, to SED.

All the data are fitted in the Wöhler plot and the R-squared value is computed using Matlab.

The method works well for the aluminum specimen, because both using Goodman and Gerber`s relation, the value of R-sqaured increases.

The R-squared is a statistic value that gives some information about the goodness of fit of a model as explained in **Errore. L'origine riferimento non è stata trovata.** and an R^2 of 1 indicates that the regression predictions perfectly fit the data.

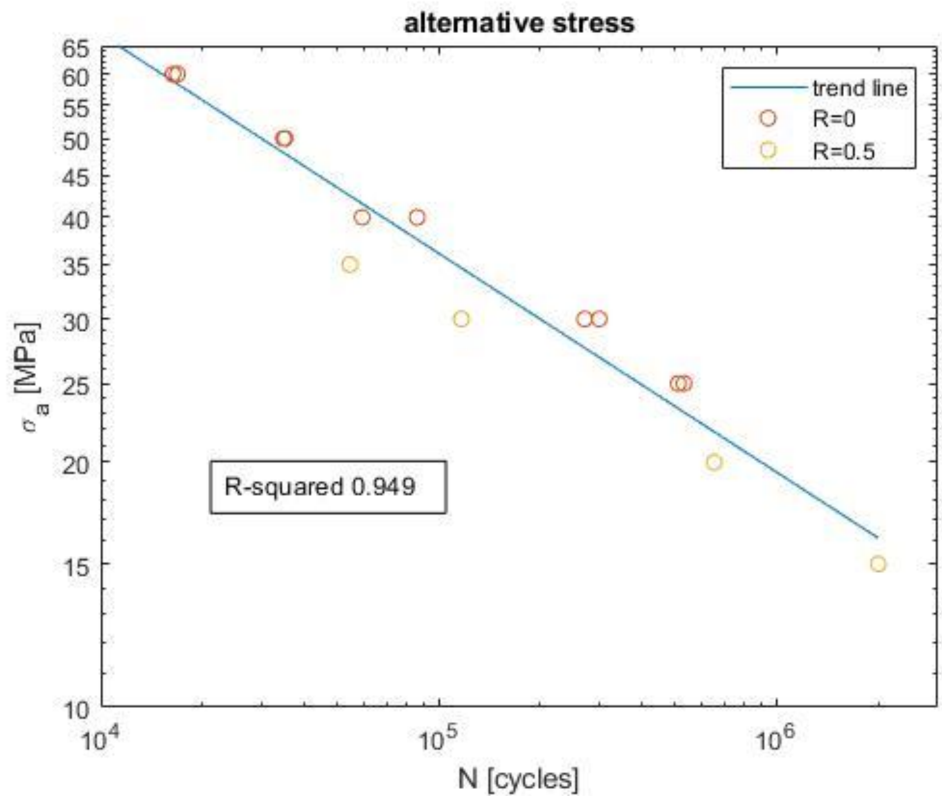

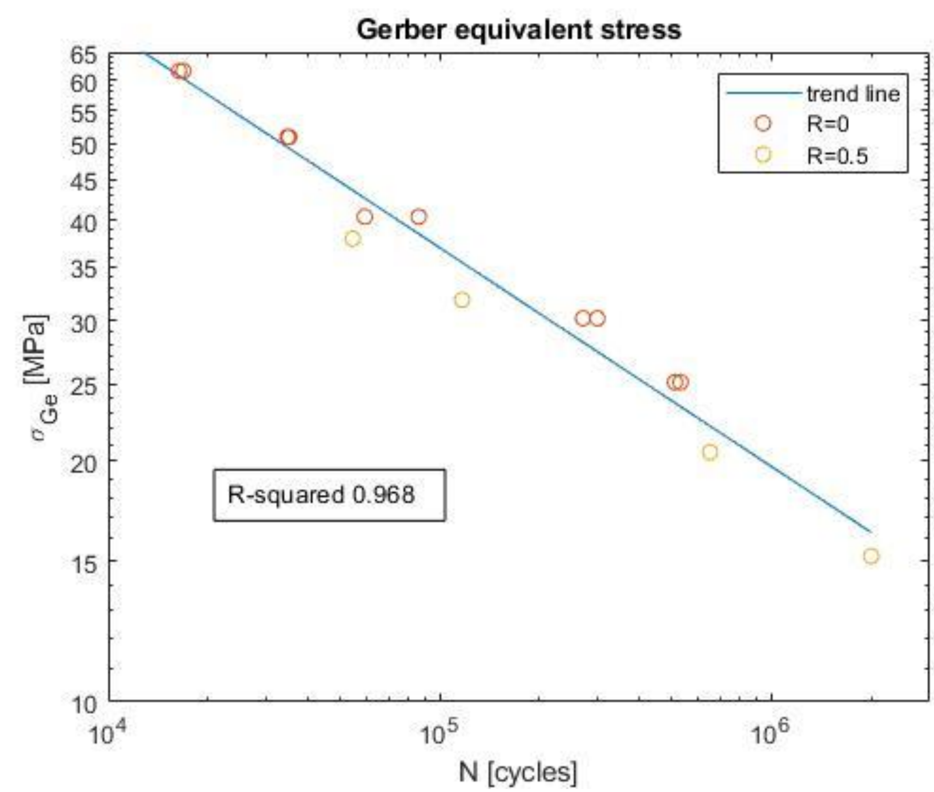

FIGURE 36 GEREBER`S RELATION ON STRESS

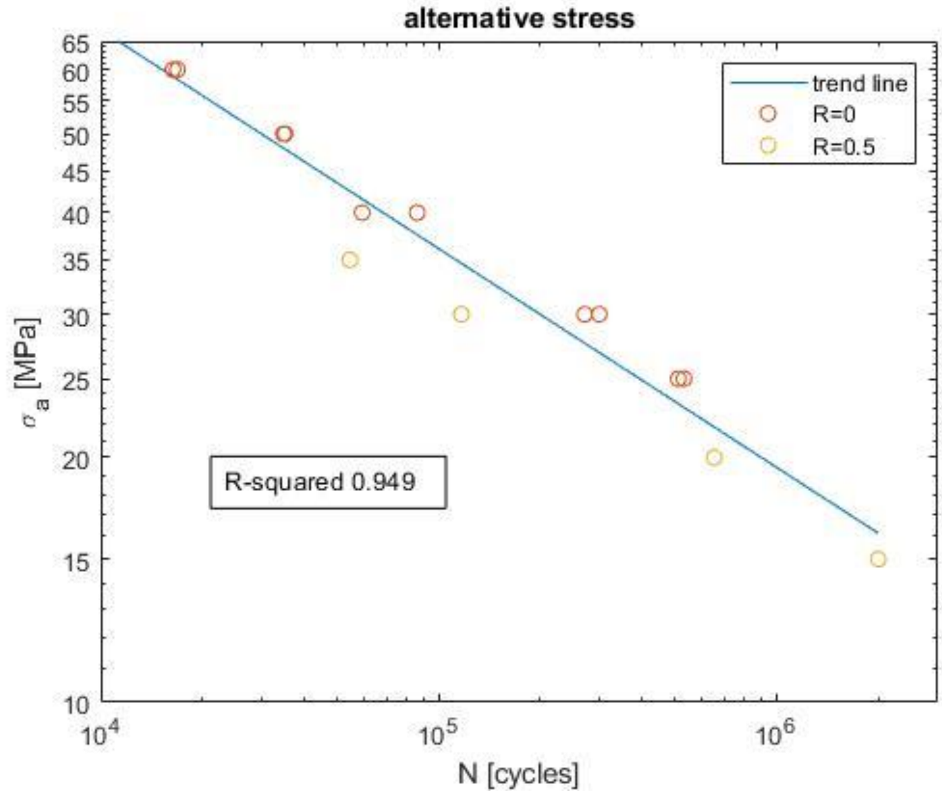

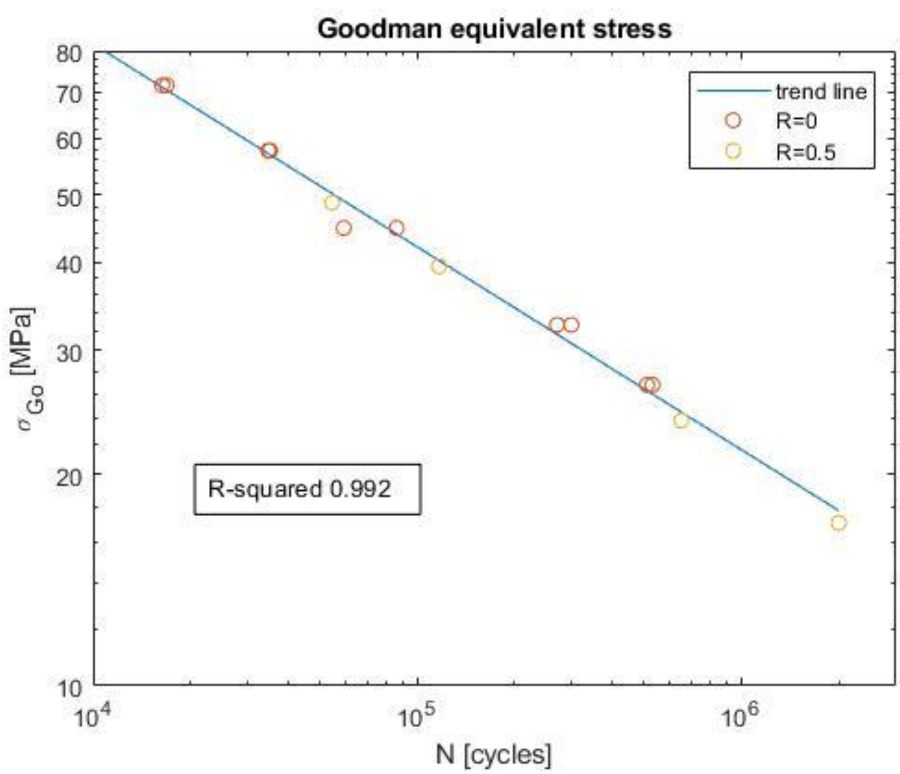

FIGURE 37 GOODMAN`S RELATION ON STRESS

The same variables defined to draw the Haigh plot are used in the following expressions and the Wöhler plot are again analyzed with SED:

$$W_m' = W_1 \sigma_m^2$$

$$W_a' = W_1 \sigma_a^2$$

$$W_u = 3.41\ Nmm/mm^3$$

$$W`_{a,Go} = \frac{W`_a}{1 - (\frac{W`_m}{W_u})}$$

$$W`_{a,Ge} = \frac{W`_a}{1 - \left(\frac{W`_m}{W_u}\right)^2}$$

Where W_1 is the value of SED when the specimen is loaded with 1 MPa at the restricted area.

For both the stress and SED there is a big advantage in using this method because in all cases the R-squared values sensibly increases, even though with SED this variance is bigger using Gerber method, while with stress is bigger using Goodman.

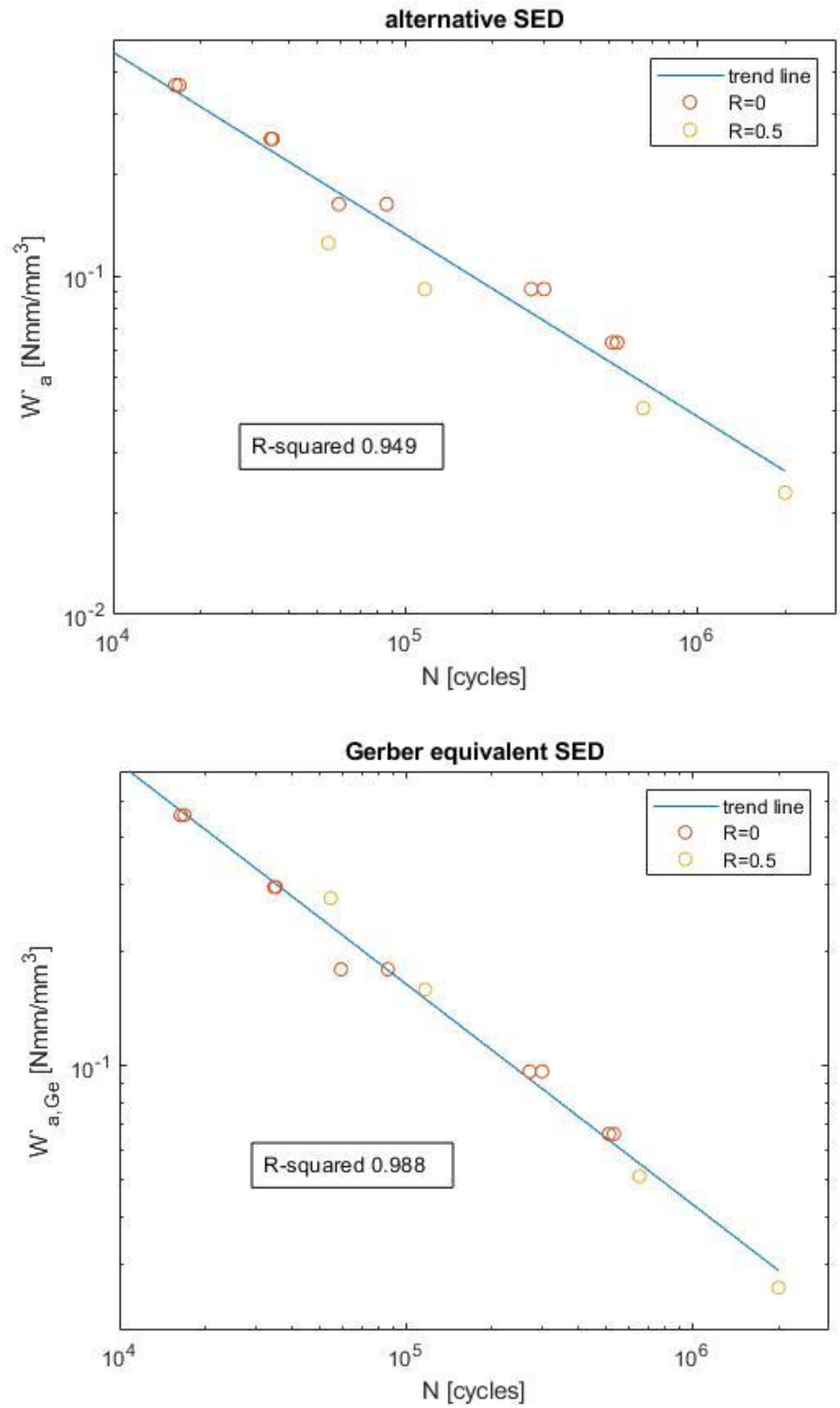

FIGURE 38 GEREBER`S RELATION ON SED

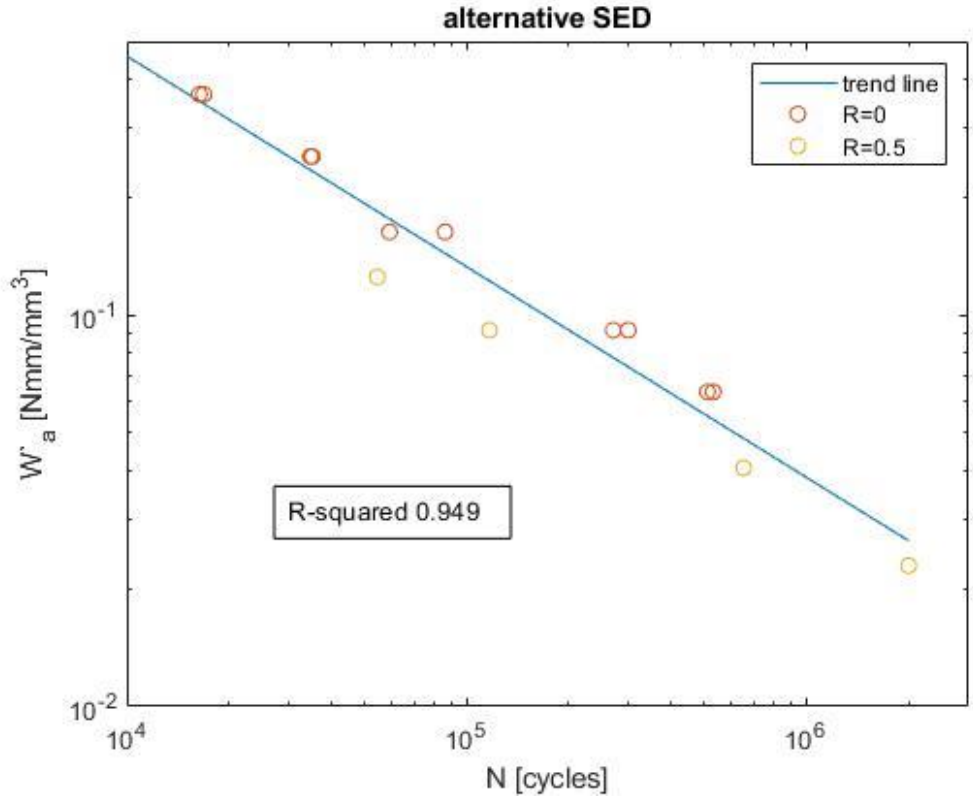

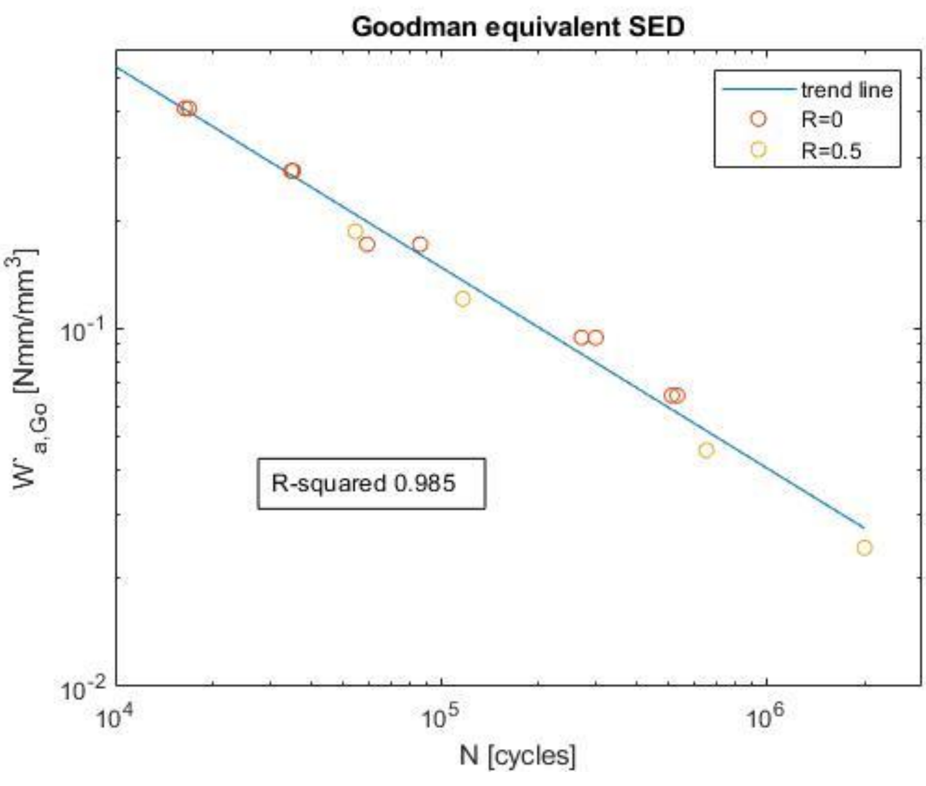

FIGURE 39 GOODMAN`S RELATION ON SED

8. Conclusion

SED method works well with the aluminum specimen and the value of the N-SIF is really close to that computed with stress, but a model with many less elements is sufficient. This is a great advantage, especially when complicated model are implemented and the computation time is much bigger than that needed for the sample, since its geometry is very simple.

For what concern the hypothesis and the simplifications adopted in this theory a particular focus on the difference between a plastic and elastic model is made.

The difference in the numerical values of SED can be quite high, and it depends a lot on the load applied to the specimen, because as it increases the region in which the material yields becomes bigger. In the plastic model the stress is limited but the strain increases and as a result the value of SED computed with this model is higher than that of the elastic one.

Anyway the method works well, as documented in the literature (10), (3), (4), and it is though possible to neglect the yield which occurs close to the notch tip, in a very restricted area. This hypothesis is very useful because it permits to use very simple models and less time consuming.

The theory works good in the Haigh diagram, in fact the precision is similar to that of the traditional Haigh diagram if the Gerber`s relation is used. For this reason SED method can be applied and once the strain energy density is computed through FEM models the new Haigh diagram can be directly used.

A particular attention is necessary in considering the variables W_m' and W_a' used in the diagram not as the actual values of the mean and alternative component of the energy, but as two equivalent parameters defined to plot a meaningful Haigh plot, in which an increase of the load ratio leads to a reduction of the component's life. Another important parameter, W_u , is defined and the point (0; W_u) is the equivalent of the (0; σ_{uts}) in the traditional Haigh diagram.

If K_{Ic} is known, an easy solution can be that of computing W_u from the well−known formula that relates SED with the mode I of N−SIF:

$$W_u = \left(\frac{K_{Ic}\, e_1}{E\, R_0^{1-\lambda_1}} \right)^2$$

In which the value of λ_1 and e_1 are those related to an opening angle of 0^o

Since K_{Ic} is not known, W_u is computed doing the mean of the value of SED at the fracturing point of all the specimen loaded with a null load ratio.

This method has also been extended to Paris theory, with the aim to predict the number of cycles necessary for the nucleation and propagation of the crack and to compute two equivalent parameters C' and n', that can be used with SED. The analytical procedure is explained in detail in the dedicated chapter, but the parameters C and n of the Paris law are taken from the literature and not directly find through the experimental procedure, so the numerical results cannot be used for practical applications.

Finally it is demonstrated that also the equivalent method devised by Badibanga, Miranda et al. works well with SED if the same parameters, W_u , W_m' and W_a' , defined for the Haigh diagram are used. Using the equivalent SED the dispersion of the experimental points from the interpolating line decreases, as it happens for the stress. In the case of the samples tested the Goodman relation works better with the stress, while with SED the Gerber relation is slightly better.

Bibliography

1. ***Livieri P, Lazzarin P., Fatigue strength of steel and aluminium welded joints based on generalised stress intensity factors and local strain energy values, Int J Fract, 2005.***

2. ***Peng Y.,Wang G.,Zhu T.,Pan S., Rong Y., Dynamic Mechanical Behaviors of 6082-T6 Aluminum Alloy, Hindawi Publishing Corporation,2013.***

3. ***Lazzarin P, Zambardi R., A finite-volume-energy based approach to predict the static and fatigue behavior of components with sharp V-shaped notches, International Journal of Fracture, 2001.***

4. ***Lazzarin P, Berto F, Zappalorto M., Rapid calculations of notch stress intensity factors based on averaged strain energy density from coarse meshes: Theoretical bases and applications, International Journal of Fatigue,2010.***

5. ***Paris P., Erdogan F., A Critical Analysis of Crack Propagation Laws,ASME,1963.***

6. ***José A.F.O. Correia, Abílio M.P. De Jesusa, Ana S.F. Alvesa, Grzegorz Lesiukb,Paulo J.S. Tavaresa, Pedro M.G.P. Moreira, Fatigue crack growth behaviour of the 6082-T6 aluminium using CT specimens with distinct notches, 21st European Conference on Fracture.*** **2016.**

7. ***Lüpfert, H.P.; Spies, H.J., Fatigue strength of heat-treated steel under static multiaxial compression stress, Adv. Eng. Mater., 2004.***

8. ***Ince A., A generalized mean stress correction model based on distortional strain,International Journal of Fatigue,2017.***

9. ***Badibanga R., Miranda T., Rocha P., Ferreira J.,da Silva C., Araújo J., The effect of mean stress on the fatigue behaviour of overhead conductor function of the H/w parameter, MATEC Web of Conferences, 2018.***

10. Lazzarin P, Berto F, Gomez F J, Zappalorto M., Some advantages derived from the use of the strain energy density over a control volume in fatigue strength assessments of welded joints, International Journal of Fatigue, 2008.

11. Radaj D. Advanced Methods of Fatigue Assessment, Springer-Verlag Berlin Heidelberg 2013.

12. ***Suresh, S., Fatigue of Materials, Cambridge University Press, 1998.***

13. ***Stephens, Ralph ,Fuchs,Henry ,Stephens,Robert, Metal Fatigue in Engineering, 2000.***

14. ***Goodman J., Mechanics Applied to Engineering, Longmans Green, 1899.***

15. ***Haigh B.P., Elastic and Fatigue Fracture in Metals. Metal Ind., 1922.***

16. ***Pallarés-Santasmartas L.,Albizuri J., Avilés A., Avilés R., Mean Stress Effect on the Axial Fatigue Strength of DIN 34CrNiMo6 Quenched and Tempered Steel, MDPI,2018.***

17. ***Marco Evangelos Biancolini, Propagazione di cricche di fatica in componenti,Phd Thesis,2015.***

18. ***Poutiainen I., Marquis G., A fatigue assessment method based on welded stress, Int J Fatigue, 2006.***